



Projected impacts of sowing date and cultivar choice on the timing of heat and drought stress in spring barley grown along a European transect

Mercy Appiah^{a,*}, Gennady Bracho-Mujica^a, Nicole C.R. Ferreira^a, Alan H. Schulman^{b,c}, Reimund P. Rötter^{a,d}

^a Tropical Plant Production and Agricultural Systems Modelling (TROPAGS), Department of Crop Sciences, Georg-August-University Göttingen, Grisebachstr 6, 37077 Göttingen, Germany

^b Natural Resources Institute Finland (Luke), Latokartanonkaari 9, FI-00790 Helsinki, Finland

^c Institute of Biotechnology and Viikki Plant Science Centre, University of Helsinki, Yliopistonkatu 3, 00014, Finland

^d Centre for Biodiversity and Sustainable Land Use (CBL), Georg-August-University Göttingen, Bispenweg 1, 37077 Göttingen, Germany

ARTICLE INFO

Keywords:

Heat and drought stress
Heading
Grain filling
Phenology shifts
Climate change adaptation
Agroclimatic indicators

ABSTRACT

Barley is one of the most important cereals for animal and human consumption. Barley heading and grain filling are especially vulnerable to heat and drought stress, which are projected to increase in the future. Therefore, site-specific adaptation options, like cultivar choice or shifting sowing dates, will be necessary. Using a global climate model ensemble and a phenology model we projected spring barley heading and maturity dates for 2031–50 for climatically contrasting sites: Helsinki (Finland), Dundee (Scotland) and Zaragoza (Spain). We compared the projected future heading and maturity dates with the baseline period (1981–2010) and described corresponding heat and drought stress conditions and how they were affected by adaptation options, i.e. shifting the sowing date by + /- 10–20 days, choosing early or late heading cultivars or combining both adaptation options, with agroclimatic indicators. At all sites and sowing dates, heading and maturity in 2031–50 occurred earlier (up to three weeks with earliest sowing) than in the baseline period. Along the European transect, the projected heading and grain filling periods were hotter than under baseline conditions but advancing heading alleviated heat stress notably. Different indicators signaled more severe drought conditions for 2031–50. At Helsinki, delayed heading periods were exposed to less drought stress, likely because the typical early summer droughts were avoided. At Zaragoza, fewer, yet more intense, rainfall events occurred during grain filling of the early cultivars. Only under scenario RCP4.5, heading and grain filling periods at Dundee were slightly wetter for the early cultivars. Our study provides a unique overview of agroclimatic conditions for heading and grain filling periods projected for 2031–50 along a climatic transect and quantifies the effects of different adaptations for spring barley. The approach can be extended by coupling the agroclimatic indicators with crop modelling.

1. Introduction

Barley is one of the most important cereals finding use in animal feeding and human consumption, e.g. in malting (Yawson et al., 2020). From 2010–2019, the European Union contributed an average of 41% to its annual global production (FAO, 2020; USDA, 2020a). As it is an internationally traded commodity, changing production conditions could not only have regional but also global implications (Newton et al., 2011; Yawson et al., 2020).

Projections show changes in climatic means and variability, which are associated with an increased frequency of extreme events, such as

heat waves, droughts, and heavy rainfall (Pendergrass et al., 2017; van der Wiel and Bintanja, 2021). In northern Europe, the sharpest surge in temperature and extreme precipitation events is expected for winter (Kovats et al., 2014; Lehtonen et al., 2014). In the Mediterranean, the strongest increase in temperature, heat waves, and dry spells, along with a notable decrease in precipitation, is projected for summer (Rötter et al., 2012; Kovats et al., 2014; Cramer et al., 2018).

Changing climate conditions have already affected crop phenology. Higher mean air temperatures have reportedly advanced the dates of phenological stages, e.g. heading and yellow ripeness, and shortened the overall growth period duration of various cereal crops (Siebert and

* Corresponding author.

E-mail address: mercy.appiah@uni-goettingen.de (M. Appiah).

<https://doi.org/10.1016/j.fcr.2022.108768>

Received 15 March 2022; Received in revised form 8 November 2022; Accepted 22 November 2022

0378-4290/© 2022 The Authors. Published by Elsevier B.V. This is an open access article under the CC BY-NC-ND license (<http://creativecommons.org/licenses/by-nc-nd/4.0/>).

Ewert, 2012; Chmielewski, 2013; Fatima et al., 2020). Reducing the exposure to heat and drought stress during vulnerable crop phases requires highly site-specific adaptation options, such as changes in sowing date or cultivar choice or a combination of both (Olesen et al., 2011; Ruiz-Ramos et al., 2018). Earlier sowing allows a crop to make use of as much winter precipitation as possible, while at the same time reducing the risk of entering heat and drought-stress prone summer periods (Sacks et al., 2010; Olesen et al., 2011). In regions like Northern Europe, where warming advances the start of the growing season and accelerates crop development, growing late-ripening cultivars is a way to counteract too-early harvests (Eitzinger et al., 2013; Fatima et al., 2020). In southern Europe, growing early-flowering cultivars could reduce the risk of exposure to terminal drought or heat stress (Yang et al., 2019). Agroclimatic indicators, e.g. temperature sum from heading until yellow ripeness (Kahiluoto et al., 2019) or number of days with water deficits in a certain time period (Trnka et al., 2011b), are valuable tools to gain a better understanding of the conditions that prevail at a specific site or grid box and to examine potential future changes (Trnka et al., 2011b; Rötter et al., 2013). Various studies have applied this approach to assess the agroclimatic growth conditions for different cereals and growing regions (Trnka et al., 2011a, 2011b; Eitzinger et al., 2013; Rivington et al., 2013; Rötter et al., 2012, 2013; Troy et al., 2015; Lüttger and Feike, 2018; Zhu and Troy, 2018; Vogel et al., 2019; Harkness et al., 2020).

However, to date, to the best of our knowledge, there is no study examining baseline and future agroclimatic conditions covering very contrasting barley production environments across Europe. Such a study would be very useful in guiding barley breeding for future conditions (e.g. Rötter et al., 2015). Here, we will examine projected changes of agroclimatic growing conditions for spring barley along a transect from Northern Europe to the Mediterranean and the impact of distinct technological adaptation options (sowing time; cultivar choice; a combination of both) with the following specific objectives:

- i) to determine whether and to what extent heading and maturity dates of early- and late-heading cultivars are projected to shift in the study period 2031–50 with or without adjusting sowing dates;
- ii) to examine how agroclimatic conditions during the heading and grain filling periods projected for 2031–50 are different from the baseline (1981–2010) with or without shifting sowing dates;
- iii) to examine the best, sowing date and cultivar choice, or specific combinations thereof, that ensure the most favorable (i.e. least exposure to heat and drought stress) agroclimatic conditions among the projections for 2031–50.

2. Materials and methods

2.1. Historical and climate change scenario data

Climate change scenario data was extracted from datasets generated by ISIMIP2b (The Inter-Sectoral Impact Model Intercomparison Project, Warszawski et al., 2014) based on CMIP5 (Taylor, 2012). This data was bias-corrected to provide long-term statistical agreement with the observation-based WATCH forcing dataset (Warszawski et al., 2014), description of the bias-correction method in Hempel et al., 2013). Its horizontal resolution was $0.5^\circ \times 0.5^\circ$ and the baseline period was 1980–2010 (Frieler et al., 2017; Warszawski et al., 2014). We extracted the bias-corrected output of an ensemble of four global climate models (GCMs) (*HadGEM2-ES*, *IPSL-CM5A-LR*, *MIROC-ESM-CHEM*, and *GFDL-ESM2M*; Frieler et al., 2017; Ito et al., 2019; Table 1) for daily maximum, minimum and mean temperature as well as precipitation for 2011–30 centered around 2020, and for 2031–50 centered around 2040 for two distinct emission scenarios. The representative concentration pathways (RCPs) 4.5 and 8.5 represented an intermediate and a very high greenhouse gas emission scenario, respectively (Pachauri and Meyer, 2015). We retrieved historical climate data from re-analysis for

Table 1

Models of the multi-model ensemble used in this study (Frieler et al., 2017; Gao et al., 2015; Warszawski et al., 2014).

Model	Model Institution	Spatial resolution (Lat. x Lon, in $^\circ$)
GDL-ESM2M	NOAA Geophysical Laboratory, USA	2.5×2.0
HadGEM2-ES	Met Office Hadley Centre, UK	1.875×1.25
IPSL-CM5A-LR	Institute Pierre-Simon-Laplace, France	3.75×1.875
MIROC-ESM-CHEM	Atmosphere and Ocean Research Institute, Tokyo	2.81×1.77

1981–2010 from the AgERA5 database (C3S, 2019) providing hourly data at a $0.1^\circ \times 0.1^\circ$ grid to characterize the baseline climate conditions at the study sites.

2.2. Climate conditions at the selected experimental sites

The observational data for this study was generated within the framework of the collaborative European, FACCE-JPI funded, SusCrop ERA-NET project “ClimBar” (“An integrated approach to evaluate and utilize genetic diversity for breeding Climate-resilient Barley”, <https://project-wheel.facejpi.net/climbar/>). The five designated study sites were located along a climatic transect from northern to southern Europe (Fig. 1A and 1B). It was assumed that the southern locations prefigure the future climate conditions at the sites further north. Two sites had to be eventually excluded from this study due to notable data gaps. The continental, cool and temperate boreal zone (BOR6) was represented by the study site near Viikki ($60^\circ 13' 30.9''\text{N}$ $25^\circ 01' 07.5''\text{E}$), roughly 10 km northeast of central Helsinki (HEL, Fig. 1A). Longforgan ($56^\circ 26' 00.6''\text{N}$ $3^\circ 07' 08.7''\text{W}$), about 14 km west of Dundee (DND), represented the Atlantic North (ATN4) with its maritime and temperate climate. Zuera ($41^\circ 51' 30.2''\text{N}$ $0^\circ 39' 15.2''\text{W}$), roughly 40 km northeast from Zaragoza (ZGZ), lies in the environmental zone labelled “Mediterranean South (MDS1)”, which describes a hot Mediterranean climate (Metzger et al., 2005, 2012). However, ZGZ is one of the cooler Mediterranean sites, as the minimum temperatures during winter can drop below 0°C (Fig. S1; Cammarano et al., 2021).

Table 2 shows the baseline conditions (1981–2010; AgEra5, C3S, 2020), during the growing season of early and late spring barley cultivars (see Section 2.3) at each site in comparison to the projected (ISI-MIP2b dataset, Warszawski et al., 2014), current (“ClimBar” trial years in comparison to current period 2011–30 are presented in Fig. S1) and future period. The projected increments of the seasonal mean temperature ($t_{\text{mean},s}$) of 3°C (HEL), 1.5°C (DND), and 0.9°C (ZGZ) along with seasonal precipitation declines of 37% (HEL), 33% (DND), and 20% (ZGZ), from the baseline to 2011–30 show that the experimental years were already subjected to climatic change.

From the baseline to 2031–50, $t_{\text{mean},s}$ increased by 3.7°C , 2.0°C , and 1.5°C at HEL, DND, and ZGZ and precipitation decreased by 35%, 33%, and 25%, respectively.

During 2011–30 and 2031–50, $t_{\text{mean},s}$ was higher under RCP8.5. During the growing season of the early cultivars at the northern sites and at ZGZ, $t_{\text{mean},s}$ was 0.2°C and 0.4°C , respectively, lower in comparison to the late cultivars. For all time slices, there was less precipitation during the growing season of the early cultivars.

2.3. Observed and projected phenological dates

Two seasons (2015/16–2016/17) of field trials, managed according to local farmers’ practices (Table S1), were conducted (weather conditions and growth season durations in Fig. S2). At each study site, a panel of more than 200 spring barley lines was sown in two replicates, whereby the northern trials were spring-sown and the southern ones winter-sown trials. The dates of heading (the day when 50% of the plot

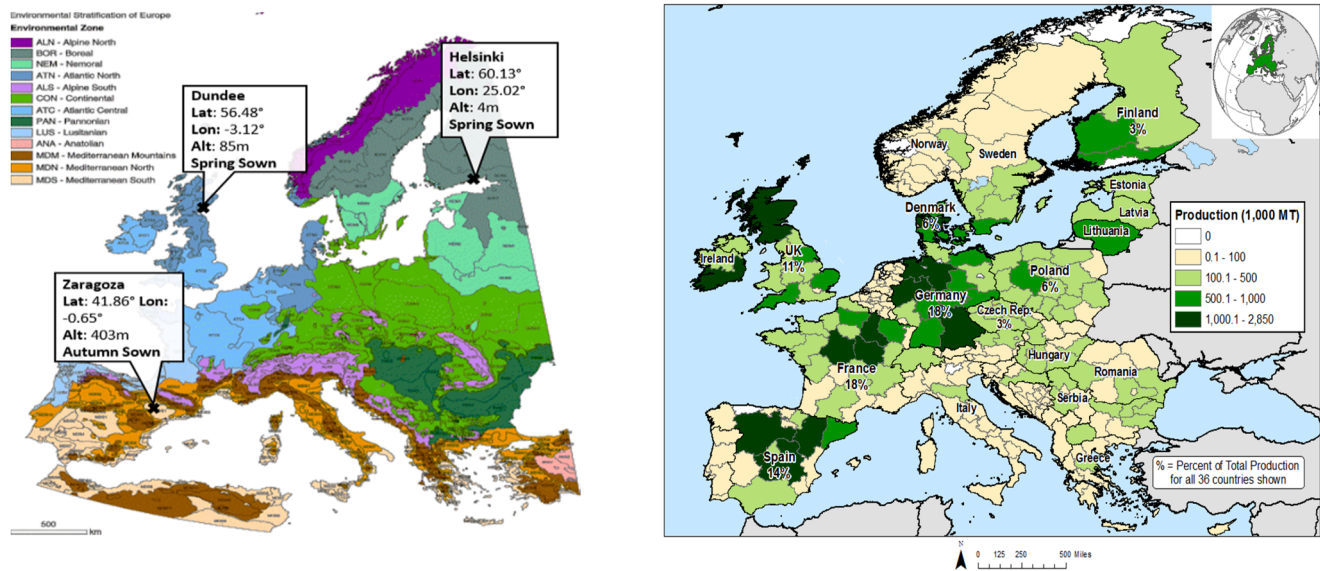


Fig. 1. A) Environmental zones and locations of the three experimental (ClimBar) sites included in this study (map from Metzger et al., 2005). B) Barley production (in 1000 million tons) in Europe (2010–2014 average; USDA, 2020b).

Table 2

Mean temperature and sum of precipitation for the growing season (sowing to maturity) of early and late spring barley cultivars as projected for the baseline (1981–2010), the current (2011–30, including ClimBar trial years), and the future (2031–50) period, for two emission scenarios (RCP4.5 and 8.5; multi-model median). Sowing = “ClimBar” sowing dates representing current farmers practice; DOY = day of year; HEL= Helsinki, DND= Dundee, ZGZ= Zaragoza.

Site	Sowing (DOY)	Cultivar Group	Baseline period (1981–2010)		RCP	Current period (2011 –2030)		Future period (2031–2050)	
			T _{mean} (°C)	Precipitation (mm)		T _{mean} (°C)	Precipitation (mm)	T _{mean} (°C)	Precipitation (mm)
HEL	136	Early	14.1	212.3	4.5	16.8	132.6	17.6	140.9
		Late	14.2	234.3	8.5	17.0	132.8	18.0	135.9
DND	82	Early	10.5	383.9	4.5	16.9	149.4	17.7	152.1
		Late	10.7	407.7	8.5	17.1	146.2	18.2	148.4
ZGZ	318	Early	9.1	237.5	4.5	11.9	263.5	12.4	262.3
		Late	9.5	250.2	8.5	12.1	253.5	12.5	254.5
		Early			4.5	12.1	280.4	12.6	279.1
		Late			8.5	12.4	269.1	12.8	268.3
		Early			4.5	10.0	188.6	10.5	178.3
		Late			8.5	10.0	189.3	10.6	174.1
		Early			4.5	10.4	204.3	10.9	192.3
		Late			8.5	10.5	203.0	11.0	189.3

have reached GS 53, i.e. 1/4 of a spike emerged, Zadoks et al., 1974) and maturity (i.e. ripeness, the day when 50% of the plot have reached GS 91, i.e. grain is difficult to divide with thumbnail, Zadoks et al., 1974) were recorded manually and weather data was collected from the on-site weather stations.

From a predefined subset of 22 cultivars, which were singled out for additional measurements for modeling and physiological analysis, we excluded those with missing data, resulting in a subset of 15 cultivars. Based on observed heading and maturity dates (Table S2) and site-specific weather data, we calculated cultivar specific thermal times for heading and maturity with a phenology model (Olesen et al., 2012, 2002):

$$S = \sum (T_i - T_b)_+ \cdot \alpha \quad (1)$$

$$\alpha = \min \left[1, \frac{(\lambda - 7)_+}{13} \right] \quad (2)$$

S is the temperature sum demand (°Cd) for the phenological phase, T_i the daily mean temperature (°C), T_b the base temperature (0 °C acc. to Rötter et al., 2011), α the photoperiodic response (Eq. 2, Olesen et al., 2002), λ is the daylength, and “+” indicates that only positive values are considered. As photoperiod mainly affects the development rate (by

accelerating it) before heading α was not considered for the time post heading (Olesen et al., 2002; Edwards, 2010).

We classified cultivars with a thermal time below the site-specific average (mean of both trial years) as early and those above as late heading cultivars (Table S2). Finally, we selected only cultivars that had the same classification across all sites (i.e. early cultivars in HEL were also early in ZGZ, etc.), resulting in nine varieties, all of which had been released between 1955 and 1996, except for cv. Binder (released in 1916).

We applied the phenology model together with the calculated thermal times and the climate data for the baseline (1981–2010), the current (2011–30), and the future (2031–50) period to estimate heading and maturity dates for each time slice. For the current and future time slices, these phenological dates were projected for both cultivar groups for each GCM x RCP combination and five sowing dates (acc. to Donatelli et al., 2015): sowing as currently implemented in “ClimBar” according to farmers’ practices; sowing 10 and 20 days earlier and later than current sowing. For the baseline period, we used only one sowing date (current farmers’ practice).

2.4. Selection and calculation of agroclimatic indicators and analysis of climate change adaptation options

The selection of agroclimatic indicators (Table 3) was limited to those representing heat and drought stress during the phenological phases of heading and grain filling, as these are the growth stages most vulnerable to environmental stress (Kadam et al., 2014; Cammarano et al., 2021). We defined the heading phase as the time from 10 days before the day of heading (GS 53, Zadoks et al., 1974) to 10 days after the day of heading, and the grain filling period as the time from the 11th day after heading to the day of maturity (i.e. ripeness, GS 91, Zadoks et al., 1974). We defined these phases based on Cossani et al. (2009), Edwards (2010), Hakala et al. (2012), Alqudah and Schnurbusch (2014), and Mirosavljević et al. (2018). Based on literature, we set different temperature thresholds for the heat stress indicators (Porter and Gawith, 1999; Hakala et al., 2012; Kahiluoto et al., 2019; Reig-Gracia et al., 2019; Jacott and Boden, 2020). Because increased temperatures accelerate crop development, hence shorten the grain filling period (Craufurd and Wheeler, 2009; Jacott and Boden, 2020), we complemented our set of indicators with “the duration of grain filling”.

The agroclimatic indicators were calculated for the baseline (1981–2010) and projected future (2031–50) heading and grain filling periods of each cultivar group. We only considered those projections in the results where at least three models agreed on the same trend. To show the overall uncertainty of the future climate projections generated by the multi-model ensemble, we calculated the multi-model mean and the standard deviation.

The presentation of hot and dry days (and later the change in the amount of rainfall) as proportional values allowed for comparisons between the different sites, set hot and dry days in relation to the considered time periods (i.e. the 21-day heading period, and grain filling periods of varying lengths), and enabled the expression of fractions of

days, thereby increasing the overall accuracy of the results. To identify the most beneficial (lowest heat or drought stress) sowing time x cultivar combination(s) (S*C) for barley production in 2031–50, we filtered those S*C that at least three GCMs agreed upon to produce the lowest (and for comparison also the highest) indicator values.

Whether the plants actually sense drought stress under limited precipitation also depends on the soil (Ludwig and Asseng, 2010). To illustrate this effect of soil, we created a representative soil water balance for each site. We used R's “sirad” package (Bojanowski, 2016) to calculate daily reference crop evapotranspiration (ET_{ref}) with the Penman-Monteith approach (Allen et al., 1998).

We calculated the daily soil water balance considering rainfall as water input and evapotranspiration as the main process removing water from the soil. Information on soil texture and the storage capacity for plant available water was gathered from the trial locations (Table 4).

For HEL and DND, we assumed soil profiles were filled to field capacity at spring sowing due to the high amounts of winter and spring precipitation (Fig. S2) and for ZGZ we assumed the soil was filled to 50% of field capacity in the potential root zone.

If the input via rainfall exceeded the maximum water storage capacity, this excess water was assumed to run off or enter the ground water. If the amount of water stored in the soil was enough to meet ET_{ref} needs then maximum evapotranspiration was possible, i.e. $ET_a = ET_{ref}$. Otherwise $ET_a < ET_{ref}$. On days with $ET_a/ET_{ref} < 0.4$ (Trnka et al., 2011b) crop growth was considered to be impaired due to water deficits. We calculated the proportional amount of water deficit days for the heading and grain filling periods, respectively, for the baseline as well as for the future time slice.

3. Results

3.1. Projected shifts of heading and maturity dates

At all three sites, the projected future temperatures were higher than the baseline level and heading and maturity advanced by a notable number of days (Fig. 2).

For all sowing dates and cultivar groups, most GCMs (except for GFDL-ESM2M) predicted earlier heading and maturity dates for 2031–50, as compared to the baseline period (Figs. 2 and 3). Overall, the projected shifts of both growth stages were slightly (1–2 days) stronger under RCP8.5. With the current sowing date, heading occurred about 2 weeks earlier in 2031–50, while maturity happened about 3 weeks earlier at HEL and DND, and about 1.5 weeks earlier at ZGZ. The earlier the sowing date, the greater the advancement of heading and maturity dates. Accordingly, the greater the delay of sowing, the smaller the advancement of heading and maturity.

Under baseline conditions, early cultivars at HEL, DND, and ZGZ entered heading 7, 10, and 18 days earlier than the late ones, respectively. Maturity of the early cultivars occurred 6–10 days ahead of the late ones. All these time differences between early and late cultivars changed by at most ± 2 days in 2031–50 (Table S3). A summary of the shifts in phenology for the different sowing dates and cultivar types considered for the three study sites is given in Fig. 4.

Table 3

Agroclimatic indicators for the heading and grain filling period selected for this study. $T_{sum,acc}$ was only calculated for the heading period.

Category	Indicator	Definition	Reference
Drought Stress	Sum of precipitation (mm)	Total sum of precipitation	Kahiluoto et al. (2019)
	Prop. of dry days (%)	Proportion of dry days (days with < 1 mm rain)	Reig-Gracia et al. (2019)
	Dry spell duration (d)	Maximum count of consecutive dry days	Reig-Gracia et al. (2019)
	Prop. of water deficit days (%)	Proportion of days with a water deficit (i.e. where $ET_a/ET_{ref} < 0.4$)	Trnka et al. (2011b)
	T_{mean} (°C)	Average temperature	Reig-Gracia et al. (2019)
Heat stress	Prop. hot days_25 (%)	Proportion of days with $t_{max} \geq 25$ °C	Hakala et al. (2012)
	Prop. hot days_28 (%)	Proportion of days with $t_{max} \geq 28$ °C	Hakala et al. (2012)
	Prop. hot days_31 (%)	Proportion of days with $t_{max} \geq 31$ °C	Kahiluoto et al. (2019)
	Duration hot spell_25 (d)	Maximum count of consecutive days with $t_{max} \geq 25$ °C	Reig-Gracia et al. (2019), Kahiluoto et al. (2019)
	Duration hot spell_28 (d)	Maximum count of consecutive days with $t_{max} \geq 28$ °C	Reig-Gracia et al. (2019), Kahiluoto et al. (2019)
	Duration hot spell_31 (d)	Maximum count of consecutive days with $t_{max} \geq 31$ °C	Reig-Gracia et al. (2019), Kahiluoto et al. (2019)
	$T_{sum,acc}$ (°C)	Sum of accumulated temperature	Hakala et al. (2012)
	Grain filling duration (d)	Duration of the grain filling period	

ET_a/ET_{ref} is the ratio of actual evapotranspiration to reference crop evapotranspiration

Table 4

Texture and water storage capacity of the soil at the selected experimental sites. For Helsinki and Dundee we assumed profiles were filled to field capacity and for Zaragoza we assumed the soil was only filled up to 50% of field capacity.

Site	Soil Texture	Maximum water storage capacity (mm)
Helsinki	Sandy loam	81
Dundee	Clay loam	245
Zaragoza	Loam	59

Maximum water storage capacity (mm) at sowing within 90 cm soil depth which was considered to be the potential rooting depth (see e.g. Brereton et al., 1986).

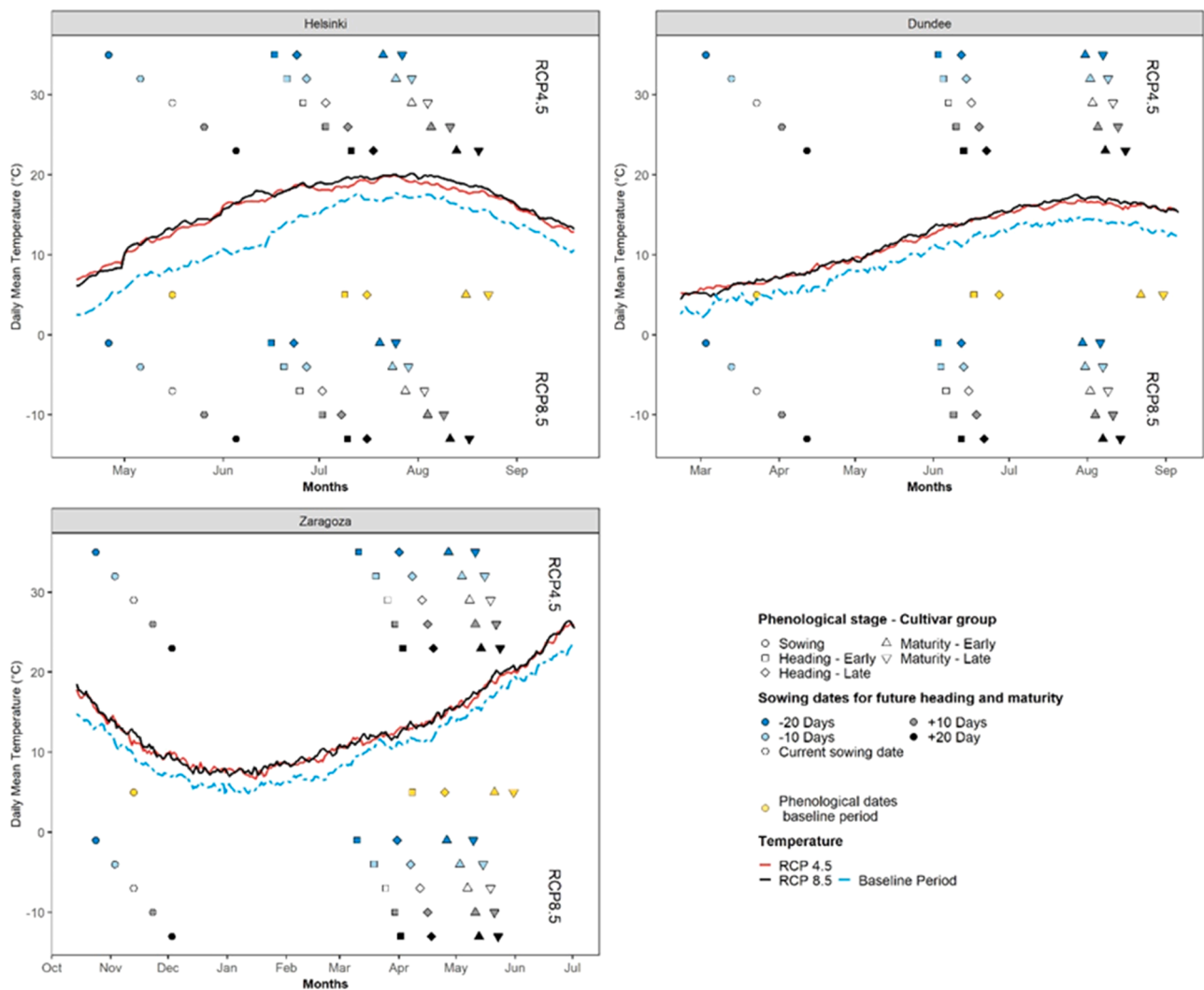


Fig. 2. Heading and maturity dates of early and late spring barley cultivars with associated mean temperatures as projected for 2031–50 (multi-model median) two emission scenarios (RCPs 4.5 and 8.5), and current, advanced (–10, –20) and delayed sowing dates (+10, +20). Baseline phenology dates and associated mean temperature (mean over 1981–2010) are presented.

Site	RCP	Cultivar group	Heading										Maturity									
			-20		-10		0		+10		+20		-20		-10		0		+10		+20	
			gfdl-esm2m	hadgem2-es	ipsi-cm5a-lr	miroc-esm-chem	gfdl-esm2m	hadgem2-es	ipsi-cm5a-lr	miroc-esm-chem	gfdl-esm2m	hadgem2-es	ipsi-cm5a-lr	miroc-esm-chem	gfdl-esm2m	hadgem2-es	ipsi-cm5a-lr	miroc-esm-chem	gfdl-esm2m	hadgem2-es	ipsi-cm5a-lr	miroc-esm-chem
HEL	4.5	Early	-20	-23	-23	-25	-16	-19	-19	-20	-11	-13	-15	-14	-4	-6	-8	-7	4	1	0	1
		Late	-20	-23	-24	-25	-16	-19	-21	-21	-11	-14	-16	-15	4	-7	-9	-8	4	1	-1	0
	8.5	Early	-19	-23	-25	-25	-16	-20	-21	-20	-10	-14	-15	-14	4	-8	-8	-8	4	-1	-1	0
		Late	-19	-24	-26	-26	-16	-21	-22	-21	-11	-16	-16	-16	-5	-9	-10	-9	4	-2	-2	-1
DND	4.5	Early	-11	-15	-16	-15	-10	-13	-14	-13	-8	-11	-12	-11	-5	-8	-9	-8	-2	-5	-5	-5
		Late	-12	-15	-17	-15	-10	-14	-15	-14	-8	-12	-13	-12	-6	-9	-10	-9	-3	-6	-7	-6
	8.5	Early	-11	-15	-18	-15	-9	-13	-16	-14	-7	-11	-14	-12	-5	-9	-11	-9	-2	-6	-7	-6
		Late	-11	-16	-19	-16	-10	-15	-17	-15	-8	-13	-15	-13	-5	-10	-12	-10	-2	-7	-8	-7
ZGZ	4.5	Early	-24	-28	-31	-30	-16	-20	-21	-21	-10	-14	-14	-13	-6	-10	-10	-9	-3	-7	-6	-6
		Late	-20	-25	-25	-25	-14	-18	-18	-18	-9	-13	-13	-12	-6	-10	-10	-9	-3	-8	-7	-6
	8.5	Early	-24	-32	-30	-31	-16	-22	-21	-21	-10	-16	-14	-15	-6	-11	-10	-10	-3	-7	-6	-7
		Late	-20	-27	-25	-26	-14	-20	-18	-19	-9	-14	-13	-14	-6	-10	-10	-10	-4	-8	-7	-8

Fig. 3. Projected shifts of spring barley heading and maturity dates at Helsinki (HEL), Dundee (DND), and Zaragoza (ZGZ) as projected by four models for 2031–50, for two emission scenarios (RCPs 4.5 and 8.5), two cultivar groups, and current (sowing time = 0), advanced (–10, –20) and delayed sowing dates (+10, +20). Red= delay, green= advancement. The color intensity highlights the magnitude of the shift.

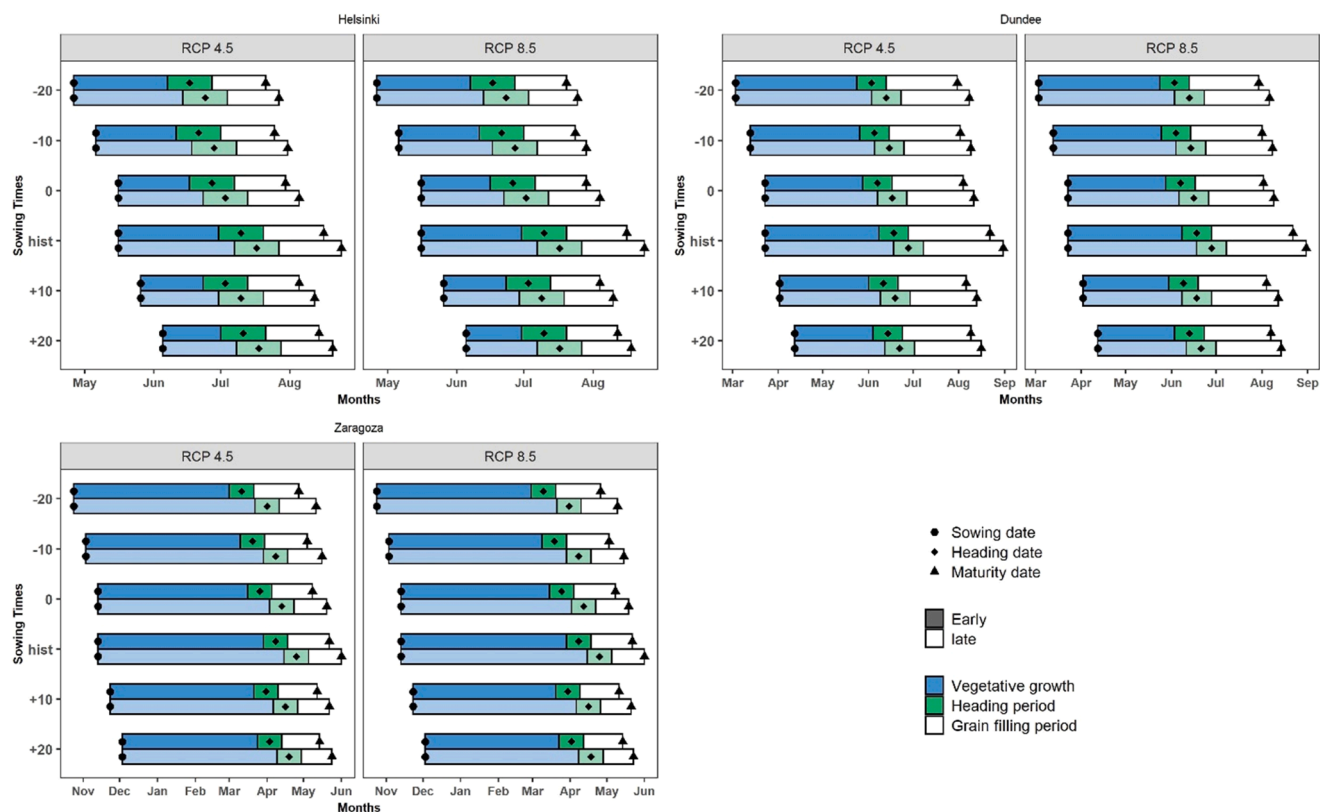


Fig. 4. Sowing, heading, and maturity dates of early and late spring barley cultivars at Helsinki, Dundee, and Zaragoza, as projected for the baseline period (1981–2010) and for 2031–50 (multi-model median), for two emission scenarios (RCPs 4.5 and 8.5) and current (sowing time = 0), advanced (–10, –20) and delayed sowing dates (+10, +20). Green bar= heading period, i.e. 10 days pre- to post-heading. White bar= grain filling period, i.e. 11th day after heading to the date of maturity. Dark bars = early cultivars, light bars= late cultivars.

3.2. Projected changes in agroclimatic conditions for early and late cultivars without sowing date adaptation

The model projections based on the current sowing date revealed notable climatic changes for heading in 2031–50, in comparison to the baseline (Fig. 5). For the north of the European transect, most drought indicators signaled a worsening of ambient conditions in 2031–50, while for the south, only the amount of precipitation changed for the worse. For all sites, the GCMs projected warmer temperatures (i.e. increases in t_{mean} , t_{sumacc} , hot days_25/28, and for *HEL* also increases in hot days_31 (RCP8.5) and hot spells_25).

According to the GCMs, the sum of precipitation during grain filling in 2030–51 decreased at all sites (Fig. 6). At the northern sites (*HEL*, *DND*-RCP8.5) dry days increased, while they decreased at the southern site. Similarly, at *HEL* dry spells got longer, yet they got shorter at *ZGZ*. The GCMs agreed on exacerbating heat stress (except for days with $t_{max} \geq 31^\circ\text{C}$) at the northern sites, especially at *HEL*. At *ZGZ*, despite the slightly lower t_{mean} (RCP8.5), the proportion of hot days increased (especially for the late cultivars).

				Drought												Heat																																																																																																																																																																																																																																																																																																																																																																																																																																																																																																																																																																																																																																																																																																																																																																																																																																																																																																																																																																																																																																																																																																											
				Sum of precipitation (%)				Prop. of dry days				Dry spell duration (d)				Tmean (°C)				Tsum acc. (°C)				Prop. of hot days_25 (%)				Prop. of hot days_28 (%)				Prop. of hot days_31 (%)				Duration hot spell_25				Duration hot spell_28				Duration hot spell_31																																																																																																																																																																																																																																																																																																																																																																																																																																																																																																																																																																																																																																																																																																																																																																																																																																																																																																																																																																																																																																																																															
Site	Sowing Time	RCP	Cultivar group	gfdl-esm2m				hadgem2-es				ipcc-cm5a-ir				gfdl-esm2m				hadgem2-es				ipcc-cm5a-ir				gfdl-esm2m				hadgem2-es				ipcc-cm5a-ir				gfdl-esm2m				hadgem2-es				ipcc-cm5a-ir				gfdl-esm2m				hadgem2-es				ipcc-cm5a-ir																																																																																																																																																																																																																																																																																																																																																																																																																																																																																																																																																																																																																																																																																																																																																																																																																																																																																																																																																																																																																																																															
				gfdl-esm2m	hadgem2-es	ipcc-cm5a-ir	microcsm-chem	gfdl-esm2m	hadgem2-es	ipcc-cm5a-ir	microcsm-chem	gfdl-esm2m	hadgem2-es	ipcc-cm5a-ir	microcsm-chem	gfdl-esm2m	hadgem2-es	ipcc-cm5a-ir	microcsm-chem	gfdl-esm2m	hadgem2-es	ipcc-cm5a-ir	microcsm-chem	gfdl-esm2m	hadgem2-es	ipcc-cm5a-ir	microcsm-chem	gfdl-esm2m	hadgem2-es	ipcc-cm5a-ir	microcsm-chem	gfdl-esm2m	hadgem2-es	ipcc-cm5a-ir	microcsm-chem	gfdl-esm2m	hadgem2-es	ipcc-cm5a-ir	microcsm-chem	gfdl-esm2m	hadgem2-es	ipcc-cm5a-ir	microcsm-chem																																																																																																																																																																																																																																																																																																																																																																																																																																																																																																																																																																																																																																																																																																																																																																																																																																																																																																																																																																																																																																																																																
HEL	0	Early	Early	-14	0	2.3	-30	5	7	7	10	2	1	1	2	0.6	1.6	2.5	2.3	24	44	63	58	15	25	35	40	4	9	3	13	0	0	0	2	0	0	0	0	0	0	0	0	0	0	0	0	0	0	0	0	0	0	0	0	0	0	0	0	0	0	0	0	0	0	0	0	0	0	0	0	0	0	0	0	0	0	0	0	0	0	0	0	0	0	0	0	0	0	0	0	0	0	0	0	0	0	0	0	0	0	0	0	0	0	0	0	0	0	0	0	0	0	0	0	0	0	0	0	0	0	0	0	0	0	0	0	0	0	0	0	0	0	0	0	0	0	0	0	0	0	0	0	0	0	0	0	0	0	0	0	0	0	0	0	0	0	0	0	0	0	0	0	0	0	0	0	0	0	0	0	0	0	0	0	0	0	0	0	0	0	0	0	0	0	0	0	0	0	0	0	0	0	0	0	0	0	0	0	0	0	0	0	0	0	0	0	0	0	0	0	0	0	0	0	0	0	0	0	0	0	0	0	0	0	0	0	0	0	0	0	0	0	0	0	0	0	0	0	0	0	0	0	0	0	0	0	0	0	0	0	0	0	0	0	0	0	0	0	0	0	0	0	0	0	0	0	0	0	0	0	0	0	0	0	0	0	0	0	0	0	0	0	0	0	0	0	0	0	0	0	0	0	0	0	0	0	0	0	0	0	0	0	0	0	0	0	0	0	0	0	0	0	0	0	0	0	0	0	0	0	0	0	0	0	0	0	0	0	0	0	0	0	0	0	0	0	0	0	0	0	0	0	0	0	0	0	0	0	0	0	0	0	0	0	0	0	0	0	0	0	0	0	0	0	0	0	0	0	0	0	0	0	0	0	0	0	0	0	0	0	0	0	0	0	0	0	0	0	0	0	0	0	0	0	0	0	0	0	0	0	0	0	0	0	0	0	0	0	0	0	0	0	0	0	0	0	0	0	0	0	0	0	0	0	0	0	0	0	0	0	0	0	0	0	0	0	0	0	0	0	0	0	0	0	0	0	0	0	0	0	0	0	0	0	0	0	0	0	0	0	0	0	0	0	0	0	0	0	0	0	0	0	0	0	0	0	0	0	0	0	0	0	0	0	0	0	0	0	0	0	0	0	0	0	0	0	0	0	0	0	0	0	0	0	0	0	0	0	0	0	0	0	0	0	0	0	0	0	0	0	0	0	0	0	0	0	0	0	0	0	0	0	0	0	0	0	0	0	0	0	0	0	0	0	0	0	0	0	0	0	0	0	0	0	0	0	0	0	0	0	0	0	0	0	0	0	0	0	0	0	0	0	0	0	0	0	0	0	0	0	0	0	0	0	0	0	0	0	0	0	0	0	0	0	0	0	0	0	0	0	0	0	0	0	0	0	0	0	0	0	0	0	0	0	0	0	0	0	0	0	0	0	0	0	0	0	0	0	0	0	0	0	0	0	0	0	0	0	0	0	0	0	0	0	0	0	0	0	0	0	0	0	0	0	0	0	0	0	0	0	0	0	0	0	0	0	0	0	0	0	0	0	0	0	0	0	0	0	0	0	0	0	0	0	0	0	0	0	0	0	0	0	0	0	0	0	0	0	0	0	0	0	0	0	0	0	0	0	0	0	0	0	0	0	0	0	0	0	0	0	0	0	0	0	0	0	0	0	0	0	0	0	0	0	0	0	0	0	0	0	0	0	0	0	0	0	0	0	0	0	0	0	0	0	0	0	0	0	0	0	0	0	0	0	0	0	0	0	0	0	0	0	0	0	0	0	0	0	0	0	0	0	0	0	0	0	0	0	0	0	0	0	0	0	0	0	0	0	0	0	0	0	0	0	0	0	0	0	0	0	0	0	0	0	0	0	0	0	0	0	0	0	0	0	0	0	0	0	0	0	0	0	0	0	0	0	0	0	0	0	0	0	0	0	0	0	0	0	0	0	0	0	0	0	0	0	0	0	0	0	0	0	0	0	0	0	0	0	0	0	0	0	0	0	0	0	0	0	0	0	0	0	0	0	0	0	0	0	0	0	0	0	0	0	0	0	0	0	0	0	0	0	0	0	0	0	0	0	0	0	0	0	0	0	0	0	0	0	0	0	0	0	0	0	0	0	0	0	0	0	0	0	0	0	0	0	0	0	0	0	0	0	0	0	0	0	0	0	0	0	0	0	0	0	0	0	0	0	0	0	0	0	0	0	0	0	0	0	0	0	0	0	0	0	0	0	0	0	0	0	0	0	0	0	0	0	0	0	0	0	0	0	0	0	0	0	0	0	0	0	0	0	0	0	0	0	0	0	0	0	0	0	0	0	0	0	0	0	0	0	0	0	0	0	0	0	0	0	0	0	0	0	0	0	0	0	0	0	0	0	0	0	0	0	0	0	0	0	0	0	0	0	0	0	0	0	0	0	0	0	0	0	0	0	0	0	0	0	0	0	0	0	0	0	0	0	0	0	0	0	0	0

Fig. 5. Changes in agroclimatic conditions during the future spring barley heading period (10 days pre- to 10 days post-heading) at Helsinki (HEL), Dundee (DND), and Zaragoza (ZGZ), as projected by four models for 2031–50, for two emission scenarios (RCPs 4.5 and 8.5) and two cultivar groups for the current sowing date (sowing time = 0). Green = positive changes (less stress), red = negative changes (more stress). The color intensity highlights the magnitude of the change. Color-coding was done for each indicator individually except for the proportions of hot days (25/28/31) which were colored as a group and so were the durations of hot spells. Prop. = proportion.

Site Sowing Time RCP Cultivar Group				Drought												Heat																																									
				Sum of precipitation (%)				Prop. of dry days (%)				Dry spell duration (d)				Tmean (°C)				Grain filling duration (d)				Prop. of hot days_25 (%)				Prop. of hot days_28 (%)				Prop. of hot days_31 (%)				Duration hot spell_25				Duration hot spell_28				Duration hot spell_31													
				gfdi-esm2m	hadgem2-es	ipci-cm5a-lr	mitoc-esm-chem	gfdi-esm2m	hadgem2-es	ipci-cm5a-lr	mitoc-esm-chem	gfdi-esm2m	hadgem2-es	ipci-cm5a-lr	mitoc-esm-chem	gfdi-esm2m	hadgem2-es	ipci-cm5a-lr	mitoc-esm-chem	gfdi-esm2m	hadgem2-es	ipci-cm5a-lr	mitoc-esm-chem	gfdi-esm2m	hadgem2-es	ipci-cm5a-lr	mitoc-esm-chem	gfdi-esm2m	hadgem2-es	ipci-cm5a-lr	mitoc-esm-chem	gfdi-esm2m	hadgem2-es	ipci-cm5a-lr	mitoc-esm-chem	gfdi-esm2m	hadgem2-es	ipci-cm5a-lr	mitoc-esm-chem	gfdi-esm2m	hadgem2-es	ipci-cm5a-lr	mitoc-esm-chem														
HEL	0	4.5	Early	-8	-26	-27	-15	3	8	8	6	1	1	1	1	0.2	2.5	3.1	3.0	0	-4	-5	-5	10	31	40	42	2	15	7	18	0	5	0	4	3	5	6	8	0	2	0	3	0	0	0	0	0	0	0							
		8.5	Late	-9	-39	-28	-16	2	12	7	8	1	1	0	2	0.9	3.2	4.1	3.6	-1	-4	-6	-5	14	37	46	44	3	18	13	19	0	5	2	6	3	6	8	8	0	2	0	3	0	0	0	0	0	0	0							
DND	0	4.5	Early	-23	-30	-25	-23	5	11	8	7	2	1	1	2	0.6	3.2	3.5	3.2	-1	-5	-6	-5	7	38	49	50	4	21	12	21	1	10	0	1	2	2	6	8	9	0	9	2	3	0	0	0	0	0	0	0						
		8.5	Late	-23	-39	-28	-26	9	14	9	8	1	1	1	1	1.2	3.9	4.0	4.1	-1	-5	-6	-6	11	43	47	56	5	23	13	23	1	10	2	2	7	7	9	0	3	2	3	0	0	0	0	0	0	0	0	0	0					
ZGZ	0	4.5	Early	-23	-30	-29	-28	-10	-3	10	3	-2	0	4	0	0.9	2.4	2.5	2.3	-3	-8	-8	-8	2	13	6	10	0	4	0	4	0	1	0	0	0	3	2	3	0	0	0	0	0	0	0	0	0	0	0	0						
		8.5	Late	-22	-31	-36	-27	-10	-2	7	1	-2	0	3	1	1.1	2.8	2.9	2.7	-4	-9	-10	-9	0	13	7	12	0	5	0	4	0	0	2	0	1	0	3	2	3	0	0	0	0	0	0	0	0	0	0	0						
		4.5	Early	-35	-37	-38	-24	-4	2	10	3	-1	1	5	1	0.9	2.7	2.9	2.6	-3	-9	-10	-8	3	13	10	12	1	4	0	2	0	1	0	0	3	2	3	0	0	0	0	0	0	0	0	0	0	0	0	0						
		8.5	Late	-34	-38	-31	-22	-4	1	6	1	-2	1	2	0	1.2	3.1	3.3	3.1	-4	-11	-11	-10	3	14	10	14	2	5	0	3	0	0	1	0	0	4	2	4	0	2	0	0	0	0	0	0	0	0	0	0						
		4.5	Early	-21	-19	-21	-13	-12	-4	5	-7	-3	0	2	-3	-0.4	0.1	-0.1	0.2	0	-1	0	-2	2	0	0	8	2	1	1	6	2	0	0	3	0	0	-1	0	0	0	2	2	0	0	0	0	0	0	0							
		8.5	Late	-20	-24	-27	-7	-16	-16	4	-8	-2	-2	3	-2	-0.2	-0.6	0.1	0.2	0	0	-1	-1	3	-5	6	6	9	-1	-5	9	0	-1	0	0	0	0	-1	1	1	0	1	0	0	0	0	0	0	0	0	0						
		4.5	Early	-25	-6	-15	-36	-9	-7	1	-4	-3	-2	0	-1	-0.2	-0.2	-0.4	0.6	0	0	0	-3	5	-2	-4	11	4	0	-3	9	0	-1	-7	0	0	0	0	0	0	0	0	0	0	0	0	0	0	0	0	0	0					
		8.5	Late	-15	-5	-19	-17	-13	-1	-7	-1	-4	-2	0	-1	-2	-2	0	-1	-0.6	0.8	0	0	-2	7	-1	-4	13	9	0	0	17	5	2	-1	13	0	0	-1	0	1	0	0	0	0	0	0	0	0	0	0	0	0	0	0	0	0

Fig. 6. Changes in agroclimatic conditions during the future spring barley grain filling period (11th day after heading to maturity) at Helsinki (HEL), Dundee (DND), and Zaragoza (ZGZ), as projected by four models for the 2031–50, for two emission scenarios (RCPs 4.5 and 8.5) and two cultivar groups for the current sowing date (sowing time = 0) Green = positive changes (less stress), red = negative changes (more stress). The color intensity highlights the magnitude of the change. Color-coding was done for each indicator individually except for the proportions of hot days (25/28/31) which were colored as a group and so were the durations of hot spells. Prop. = proportion.

3.3. Projected agroclimatic conditions for early versus late cultivars

Fig. 7 depicts the contrast between agroclimatic conditions projected for the early versus the late cultivars during heading in 2031–50 only considering the current sowing date. For each site, different indicators described a drier climatic environment for the early than for the late cultivars, i.e. less rain (at DND only under RCP8.5), longer dry spells (ZGZ-RCP8.5), and more dry days (HEL, ZGZ). Only for RCP4.5 at DND, the models projected fewer dry days for the early than for the late cultivars. According to most indicators, cooler conditions prevailed for the early cultivars, at all sites, i.e. lower t_{mean} , and t_{sumacc} , fewer hot days 25 (in HEL only under RCP8.5 and in DND only under RCP4.5) and at ZGZ fewer hot days 28/31.

While the GCMs projected more rain for grain filling of the early cultivars (HEL - RCP8.5, DND RCP4.5, ZGZ), they also indicated more dry days (DND, ZGZ both under RCP8.5) and longer dry spells (DND -RCP8.5, ZGZ) for the early as compared to the late cultivars (Fig. 8). Most indicators suggested cooler growth conditions for the early cultivars, whereby a difference for hot spells and hot days_31 only occurred at ZGZ.

3.4. Climate change adaptation by shifting the sowing date

Here, the effects of changing the sowing date are presented independently of the cultivar type. Shifting the sowing date changed the projected growing conditions during heading (Fig. 9 and Fig. S3). At HEL

and ZGZ, advancing sowing resulted in a drier (lower precipitation, more dry days) and, at all three sites, a cooler climatic environment (lower t_{mean} and t_{sumacc} and, at ZGZ, less hot days 25/28) than when sowing as currently. For each case, the opposite was true for delayed sowing.

The trend for projected grain filling in 2031–50 was towards lower t_{mean} with advanced sowing (at all sites), but higher t_{mean} with delayed sowing (DND, ZGZ; Fig. 10; Fig. S4). In some cases, the number of hot days (with $t_{max} \geq 25^\circ\text{C}$ at HEL, ZGZ; $t_{max} \geq 28^\circ\text{C}$ at HEL, ZGZ; $t_{max} \geq 31^\circ\text{C}$ at ZGZ) and the duration of hot spells (with $t_{max} \geq 25^\circ\text{C}$ at ZGZ, sowing -20) decreased with earlier sowing. A delay of sowing changed the projections for hot days at ZGZ in the opposite direction. At HEL (RCP4.5), conditions got drier with earlier sowing (less rainfall, more dry days at sowing -20) and wetter with delayed sowing. At ZGZ, sowing 10 days earlier resulted in higher rainfall, while the opposite was true for sowing 20 days later. The dry spell duration increased when sowing was advanced by 20 days.

3.5. Climate change adaptation by combining cultivar choice and shifts in sowing date

Fig. 11 and Fig. S5 highlight the sowing by cultivar combinations (S^*Cs) for which at least three GCMs projected the lowest or highest indicator values for heading in 2031–50 (also see Section 2.4). These values indicated those S^*Cs that caused the least or most drought/heat stress exposure. At HEL and ZGZ, sowing early cultivars 20 days earlier

Site	Sowing Time	Cultivar group	RCP	Drought												Heat																																																																																																																																																																																																																																																																																																																																																																																																																																																																																																																																																																																																																																																																																																																																																																																																																																																																																																																																																																																																																																																																																																																																																																																																																									
				Sum of precipitation (early: %, late: mm)				Prop. of dry days (%)				Dry spell duration (d)				Tmean (°C)				Tsum acc. (°C)				Prop. of hot days_25 (%)				Prop. of hot days_28 (%)				Prop. of hot days_31 (%)				Duration hot spell_25 (d)				Duration hot spell_28 (d)				Duration hot spell_31 (d)																																																																																																																																																																																																																																																																																																																																																																																																																																																																																																																																																																																																																																																																																																																																																																																																																																																																																																																																																																																																																																																																																																																																																																																													
				gfdi-esm2m	hadgem2-es	ipci-cm5a-lr	mitoc-esm-chem	gfdi-esm2m	hadgem2-es	ipci-cm5a-lr	mitoc-esm-chem	gfdi-esm2m	hadgem2-es	ipci-cm5a-lr	mitoc-esm-chem	gfdi-esm2m	hadgem2-es	ipci-cm5a-lr	mitoc-esm-chem	gfdi-esm2m	hadgem2-es	ipci-cm5a-lr	mitoc-esm-chem	gfdi-esm2m	hadgem2-es	ipci-cm5a-lr	mitoc-esm-chem	gfdi-esm2m	hadgem2-es	ipci-cm5a-lr	mitoc-esm-chem	gfdi-esm2m	hadgem2-es	ipci-cm5a-lr	mitoc-esm-chem	gfdi-esm2m	hadgem2-es	ipci-cm5a-lr	mitoc-esm-chem																																																																																																																																																																																																																																																																																																																																																																																																																																																																																																																																																																																																																																																																																																																																																																																																																																																																																																																																																																																																																																																																																																																																																																																																		
HEL	0	Early	4.5	-15.6	-8.3	-4.3	-26.2	4	1	0	5	2	0	1	0.0	-0.5	0.0	-0.4	1	-10	0	-8	4	-3	-5	-1	2	-2	1	-2	0	-1	0	0	0	0	0	0	0	0	0	0	0	0	0	0	0	0	0	0	0	0	0	0	0	0	0	0	0	0	0	0	0	0	0	0	0	0	0	0	0	0	0	0	0	0	0	0	0	0	0	0	0	0	0	0	0	0	0	0	0	0	0	0	0	0	0	0	0	0	0	0	0	0	0	0	0	0	0	0	0	0	0	0	0	0	0	0	0	0	0	0	0	0	0	0	0	0	0	0	0	0	0	0	0	0	0	0	0	0	0	0	0	0	0	0	0	0	0	0	0	0	0	0	0	0	0	0	0	0	0	0	0	0	0	0	0	0	0	0	0	0	0	0	0	0	0	0	0	0	0	0	0	0	0	0	0	0	0	0	0	0	0	0	0	0	0	0	0	0	0	0	0	0	0	0	0	0	0	0	0	0	0	0	0	0	0	0	0	0	0	0	0	0	0	0	0	0	0	0	0	0	0	0	0	0	0	0	0	0	0	0	0	0	0	0	0	0	0	0	0	0	0	0	0	0	0	0	0	0	0	0	0	0	0	0	0	0	0	0	0	0	0	0	0	0	0	0	0	0	0	0	0	0	0	0	0	0	0	0	0	0	0	0	0	0	0	0	0	0	0	0	0	0	0	0	0	0	0	0	0	0	0	0	0	0	0	0	0	0	0	0	0	0	0	0	0	0	0	0	0	0	0	0	0	0	0	0	0	0	0	0	0	0	0	0	0	0	0	0	0	0	0	0	0	0	0	0	0	0	0	0	0	0	0	0	0	0	0	0	0	0	0	0	0	0	0	0	0	0	0	0	0	0	0	0	0	0	0	0	0	0	0	0	0	0	0	0	0	0	0	0	0	0	0	0	0	0	0	0	0	0	0	0	0	0	0	0	0	0	0	0	0	0	0	0	0	0	0	0	0	0	0	0	0	0	0	0	0	0	0	0	0	0	0	0	0	0	0	0	0	0	0	0	0	0	0	0	0	0	0	0	0	0	0	0	0	0	0	0	0	0	0	0	0	0	0	0	0	0	0	0	0	0	0	0	0	0	0	0	0	0	0	0	0	0	0	0	0	0	0	0	0	0	0	0	0	0	0	0	0	0	0	0	0	0	0	0	0	0	0	0	0	0	0	0	0	0	0	0	0	0	0	0	0	0	0	0	0	0	0	0	0	0	0	0	0	0	0	0	0	0	0	0	0	0	0	0	0	0	0	0	0	0	0	0	0	0	0	0	0	0	0	0	0	0	0	0	0	0	0	0	0	0	0	0	0	0	0	0	0	0	0	0	0	0	0	0	0	0	0	0	0	0	0	0	0	0	0	0	0	0	0	0	0	0	0	0	0	0	0	0	0	0	0	0	0	0	0	0	0	0	0	0	0	0	0	0	0	0	0	0	0	0	0	0	0	0	0	0	0	0	0	0	0	0	0	0	0	0	0	0	0	0	0	0	0	0	0	0	0	0	0	0	0	0	0	0	0	0	0	0	0	0	0	0	0	0	0	0	0	0	0	0	0	0	0	0	0	0	0	0	0	0	0	0	0	0	0	0	0	0	0	0	0	0	0	0	0	0	0	0	0	0	0	0	0	0	0	0	0	0	0	0	0	0	0	0	0	0	0	0	0	0	0	0	0	0	0	0	0	0	0	0	0	0	0	0	0	0	0	0	0	0	0	0	0	0	0	0	0	0	0	0	0	0	0	0	0	0	0	0	0	0	0	0	0	0	0	0	0	0	0	0	0	0	0	0	0	0	0	0	0	0	0	0	0	0	0	0	0	0	0	0	0	0	0	0	0	0	0	0	0	0	0	0	0	0	0	0	0	0	0	0	0	0	0	0	0	0	0	0	0	0	0	0	0	0	0	0	0	0	0	0	0	0	0	0	0	0	0	0	0	0	0	0	0	0	0	0	0	0	0	0	0	0	0	0	0	0	0	0	0	0	0	0	0	0	0	0	0	0	0	0	0	0	0	0	0	0	0	0	0	0	0	0	0	0	0	0	0	0	0	0	0	0	0	0	0	0	0	0	0	0	0	0	0	0	0	0	0	0	0	0	0	0	0	0	0	0	0	0	0	0	0	0	0	0	0	0	0	0	0	0	0	0	0	0	0	0	0	0	0	0	0	0	0	0	0	0	0	0	0	0	0	0	0	0	0	0	0	0	0	0	0	0	0	0	0	0	0	0	0	0	0	0	0	0	0	0	0	0	0	0	0	0	0	0	0	0	0	0	0	0	0	0	0	0	0	0	0	0	0	0	0	0	0	0	0	0	0	0	0	0	0	0	0	0	0	0	0	0	0	0	0	0	0	0	0	0	0	0	0	0	0	0	0	0	0	0	0	0	0	0	0	0	0	0	0	0	0	0	0	0	0	0	0	0	0	0	0	0	0	0	0	0	0	0	0	0	0	0	0	0	0	0	0	0	0	0	0	0	0	0	0	0	0	0	0	0	0	0	0	0	0	0	0	0	0	0	0	0	0	0	0	0	0	0	0	0	0	0	0	0	0	0	0	0	0	0	0	0	0	0	0	0	0	0	0	0	0	0	0	0	0	0	0	0	0	0	0	0	0	0	0	0	0	0	0	0	0	0	0	0	0	0	0	0	0	0	0	0	0	0	0	0	0	0	0	0	0	0	0

Fig. 7. Agroclimatic conditions during the future spring barley heading period (10 days pre- to 10 days post- heading) at Helsinki (HEL), Dundee (DND) and Zaragoza (ZGZ) as projected by four models for 2031–50, for two emission scenarios (RCPs 4.5 and 8.5) and the current sowing date (0), for the late (absolute values in the given units) and early cultivars (values presented as difference to late cultivars). Green = positive change (less stress), red = negative change (more stress). The intensity of the color highlights the magnitude of the change. Color-coding was done for each indicator individually except for the proportions of hot days (25/28/31) which were colored as a group and so were the durations of hot spells. Prop. = proportion.

Site	Sowing Time	Cultivar group	RCP	Drought												Heat											
				Sum of precipitation (early: %, late: mm)				Prop. of dry days (%)				Dry spell duration (d)				Tmean (°C)				Grain filling duration (d)				Prop. of hot days_25 (%)			
				gfdi-esm2m	hadgem2-es	ipoi-cm5a-lr	micro-esm-chem	gfdi-esm2m	hadgem2-es	ipoi-cm5a-lr	micro-esm-chem	gfdi-esm2m	hadgem2-es	ipoi-cm5a-lr	micro-esm-chem	gfdi-esm2m	hadgem2-es	ipoi-cm5a-lr	micro-esm-chem	gfdi-esm2m	hadgem2-es	ipoi-cm5a-lr	micro-esm-chem	gfdi-esm2m	hadgem2-es	ipoi-cm5a-lr	micro-esm-chem
HEL	0	Early	4.5	0.0	20.0	0.0	0.0	2	3	2	-1	0	0	1	-1	-0.2	-0.2	-0.5	-0.1	1	0	1	0	-2	-4	-4	0
			8.5	8.8	13.3	-1.8	1.8	5	-2	0	0	1	0	0	1	-0.1	-0.2	0.0	-0.4	0	0	0	1	-2	-3	-4	-4
		Late	4.5	67	45	53	62	67	45	53	64	8	8	7	9	17.4	19.7	20.6	20.1	26	23	21	22	18	41	50	48
			8.5	57	45	56	55	65	70	65	64	8	8	8	8	17.7	20.4	20.5	20.6	26	22	21	21	15	47	51	60
DND	0	Early	4.5	0.9	5.3	-1.1	1.0	0	-1	3	2	0	0	1	-1	-0.2	-0.4	-0.4	-0.5	2	2	3	2	1	-1	-2	-3
			8.5	2.2	4.7	-7.4	0.0	0	1	4	2	1	0	3	1	-0.3	-0.4	-0.4	-0.5	2	3	2	3	-1	-2	-1	-3
		Late	4.5	108	95	88	101	44	52	61	55	7	9	12	10	15.0	16.7	16.8	16.6	49	44	43	44	4	14	8	13
			8.5	91	86	95	108	50	55	60	55	7	9	10	11	15.1	17.0	17.2	17.7	49	44	42	43	1	15	11	15
ZGZ	0	Early	4.5	27.3	2.4	-10.0	21.1	2	10	-1	-1	1	4	1	1	-2.7	-1.3	-2.2	-2.0	7	6	8	6	-14	-8	-18	-11
			8.5	14.3	28.2	4.7	0.0	2	2	3	1	1	2	2	2	-2.1	-2.0	-1.8	-1.2	7	7	7	6	-15	-16	-13	-15
		Late	4.5	33	42	30	38	60	60	80	68	8	8	13	8	16.7	16.3	17.0	17.1	27	27	26	26	20	10	16	20
			8.5	35	39	43	34	63	65	72	69	8	8	10	9	16.8	16.7	16.3	17.7	27	27	27	25	20	15	11	28

Fig. 8. Agroclimatic conditions during the future spring barley grain filling period (11th day after heading to maturity) at Helsinki (HEL), Dundee (DND) and Zaragoza (ZGZ) as projected by four models for 2031–50, for two emission scenarios (RCPs 4.5 and 8.5) and the current sowing date (0), for the late (absolute values in the given units) and early cultivars (values presented as difference to late cultivars). Green = positive change (less stress), red = negative change (more stress). The intensity of the color highlights the magnitude of the change. Color-coding was done for each indicator individually except for the proportions of hot days (25/28/31) which were colored as a group and so were the durations of hot spells. Prop. = proportion.

Sowing Time	RCP	Cultivar group	Drought												Zaragoza											
			Sum of precipitation (sowing -/+ 10/20 in %; sowing 0 in mm)				Prop. of dry days (%)				Dry spell duration (d)				Tmean (°C)				Tsum acc. (°C)				Prop. of hot days_25 (%)			
			gfdi-esm2m	hadgem2-es	ipoi-cm5a-lr	micro-esm-chem	gfdi-esm2m	hadgem2-es	ipoi-cm5a-lr	micro-esm-chem	gfdi-esm2m	hadgem2-es	ipoi-cm5a-lr	micro-esm-chem	gfdi-esm2m	hadgem2-es	ipoi-cm5a-lr	micro-esm-chem	gfdi-esm2m	hadgem2-es	ipoi-cm5a-lr	micro-esm-chem	gfdi-esm2m	hadgem2-es	ipoi-cm5a-lr	micro-esm-chem
-20	4.5	Early	-26.3	-21.1	-9.1	-23.8	5	2	3	6	1	1	1	1	-1.0	-1.1	-0.9	-1.1	-21	-22	-18	-23	-5	-6	-2	-5
			-8.0	-12.5	-19.2	-10.7	3	2	1	-2	0	-1	0	1	-0.6	-1.0	-0.8	-1.1	-13	-20	-18	-28	-3	-5	-2	-10
		Late	0.0	-12.0	-46.7	-5.6	1	3	-7	1	-1	1	-3	1	-1.0	-1.2	-1.2	-1.6	-21	-24	-27	-31	-3	-6	-2	-8
			-13.6	-16.1	-28.6	-5.0	3	6	7	0	2	1	2	0	-0.8	-1.1	-0.6	-1.1	-17	-23	-12	-24	-1	-3	-4	-6
-10	4.5	Early	-15.8	-10.5	-4.5	-19.0	3	2	2	4	1	1	0	1	-0.4	-0.3	-0.3	-0.5	-8	-6	-6	-10	-1	-2	-1	-3
			0.0	-4.2	-7.7	0.0	-1	0	0	-1	0	-1	0	0	-0.3	-0.5	-0.3	-0.7	-7	-10	-7	-13	-2	-3	-1	-4
		Late	-5.6	-4.0	15.4	-5.6	1	1	-3	1	0	1	-1	0	-0.4	-0.4	-0.3	-0.6	-9	-7	-9	-14	-2	-2	0	-3
			-9.1	-6.5	-19.0	5.0	2	3	5	0	1	1	1	-1	-0.4	-0.6	-0.3	-0.6	-8	-13	-5	-12	0	-2	-2	-3
0	4.5	Early	19	19	22	21	73	80	79	67	10	11	11	8	12.4	13.0	12.3	12.4	260	273	258	260	12	8	4	9
			25	24	26	28	64	76	78	66	8	11	11	7	13.4	14.3	13.6	14.1	282	299	286	295	17	16	7	21
		Late	18	25	13	18	74	75	88	71	11	9	14	10	12.4	12.6	12.8	12.8	261	264	270	269	13	9	4	15
			22	31	21	20	68	67	80	69	8	8	11	9	13.7	13.9	13.7	14.4	287	292	287	302	17	13	9	23
+10	4.5	Early	10.5	5.3	0.0	14.3	-4	-1	0	-2	-1	-1	0	0	0.2	0.2	0.3	0.3	5	5	6	7	1	2	0	3
			0.0	0.0	0.0	0.0	0	-1	0	1	0	0	0	1	0.3	0.3	0.3	0.4	6	8	6	10	1	3	2	3
		Late	5.6	4.0	7.7	13.1	-2	-2	-1	-2	-1	0	0	-1	0.2	0.2	0.3	0.4	4	4	5	8	2	1	1	2
			4.5	3.2	9.5	0.0	-1	0	-2	0	0	0	0	0	0.2	0.3	0.2	0.4	6	7	6	9	1	1	2	3
+20	4.5	Early	21.1	15.8	0.0	19.0	-6	-2	0	-2	-1	-1	0	0	0.4	0.4	0.5	0.6	8	9	12	13	2	3	1	5
			0.0	4.2	0.0	0.0	0	-2	1	2	0	0	0	1	0.6	0.5	0.6	0.8	12	13	13	18	1	3	4	6
		Late	5.6	12.0	15.4	11.1	-2	-4	-1	-3	-1	0	-1	-2	0.4	0.4	0.4	0.6	8	9	8	13	3	2	2	3
			4.5	0.0	19.0	0.0	-2	1	-4	0	-1	0	-1	0	0.5	0.6	0.4	0.7	10	12	9	16	1	2	3	5

Fig. 9. Agroclimatic conditions during the future spring barley heading period (10 days pre- to 10 days post- heading) at Zaragoza as projected by four models for 2031–50, for two emission scenarios (RCPs 4.5 and 8.5) and two cultivar groups. The values for the advanced (−10, −20) and delayed (+10, +20) sowing dates indicate the projected change from the current sowing date (absolute values in the given units). Green = positive changes, red = negative changes. The intensity of the color highlights the magnitude of the change. Color-coding was done for each indicator individually except for the proportions of hot days (25/28/31) which were colored as a group and so were the durations of hot spells.

created the driest ambient conditions. For this particular S°C combination, the GCMs projected more dry days, less precipitation, and longer dry spells (ZGZ – RCP4.5: early-10) than for all other S°Cs.

The projections for the wettest conditions (i.e. least drought stress) depended on the RCP, e.g. for HEL, the GCMs projected the most rainfall under RCP4.5, for late cultivars sown 20 days later, but under RCP 8.5 for early cultivars sown 20 days later. At ZGZ, dry spells were shortest for late cultivars sown 10 days earlier under RCP4.5, yet, under RCP8.5 they were shortest for late cultivars sown 20 days later.

For all sites, the coolest climatic conditions were projected for early cultivars sown 20 days earlier, i.e. t_{mean} and t_{sum_acc} , and at DND and ZGZ also the number of hot days and the hot spell duration, were lowest. The GCMs agreed on the hottest conditions for late cultivars sown 20 days later.

Regarding drought stress during grain filling, again the results differed between the RCPs. For example, at ZGZ (Fig. 12), the most rainfall was projected for early cultivars sown 10 days earlier (RCP4.5) and the least for late cultivars sown 20 days later (RCP4.5). At DND, for each drought indicator, a different S°C created the most favorable

conditions (Fig. S5).

For HEL, the heat indicators show the lowest values (coolest conditions) for early cultivars sown 20 days earlier, except for hot days_25 and hot spells_25 which both reached their minima for late cultivars sown 20 days later. Under RCP4.5, the highest t_{mean} , highest proportion of hot days_25, and longest hot spell_25 were projected for late cultivars sown 10 days in advance.

For DND and ZGZ, the heat indicators agreed on the coolest conditions for early cultivars sown 20 days in advance and the warmest for late cultivars sown 20 days later.

3.6. Exemplary calculation of water deficit days

We calculated the proportion of water deficit days using the soils representative for the study sites. In the baseline period, only up to 6% of the days during heading and grain filling were classified as water deficit days at HEL and ZGZ (Table S6). For 2031–50, the models projected a decline to almost 0% water deficit days during heading and grain filling of early and late cultivars at ZGZ (Fig. S10, Fig. S11 - sowing 0). Neither

			Zaragoza																																																																																																																																																																																																																																																																																																																																																																																																																																																																																																																																																																																																																																																																																																																																																																																																																																																																																																																																																																																																															
			Drought												Heat																																																																																																																																																																																																																																																																																																																																																																																																																																																																																																																																																																																																																																																																																																																																																																																																																																																																																																																																																																																																			
			Sum of precipitation sowing -/+ 10/20 in %; sowing 0 in mm				Prop. of dry days (%)				Dry spell duration (d)				Tmean (°C)				Grain filling duration (d)				Prop. of hot days_25 (%)				Prop. of hot days_28 (%)				Prop. of hot days_31 (%)				Duration hot spell_25 (d)				Duration hot spell_28 (d)				Duration hot spell_31 (d)																																																																																																																																																																																																																																																																																																																																																																																																																																																																																																																																																																																																																																																																																																																																																																																																																																																																																																																																																																							
			gdl-esm2m hadgem2-es ipsi-cm5a-lr micro-esm-chem				gdl-esm2m hadgem2-es ipsi-cm5a-lr micro-esm-chem				gdl-esm2m hadgem2-es ipsi-cm5a-lr micro-esm-chem				gdl-esm2m hadgem2-es ipsi-cm5a-lr micro-esm-chem				gdl-esm2m hadgem2-es ipsi-cm5a-lr micro-esm-chem				gdl-esm2m hadgem2-es ipsi-cm5a-lr micro-esm-chem				gdl-esm2m hadgem2-es ipsi-cm5a-lr micro-esm-chem				gdl-esm2m hadgem2-es ipsi-cm5a-lr micro-esm-chem				gdl-esm2m hadgem2-es ipsi-cm5a-lr micro-esm-chem				gdl-esm2m hadgem2-es ipsi-cm5a-lr micro-esm-chem																																																																																																																																																																																																																																																																																																																																																																																																																																																																																																																																																																																																																																																																																																																																																																																																																																																																																																																																																																											
Sowing Time	RCP	Cultivar group	4.8	-4.7	9.5	-2.2	4	6	-1	-1	1	2	0	1	-1.1	-1.0	-1.6	-1.3	4	3	4	3	-4	-5	-12	-9	-2	-2	-5	-5	-1	-1	-1	-1	-1	-1	-1	-1	-1	-1	-1	-1	-1	-1	-1	-1	-1	-1	-1	-1	-1	-1	-1	-1	-1	-1	-1	-1	-1	-1	-1	-1	-1	-1	-1	-1	-1	-1	-1	-1	-1	-1	-1	-1	-1	-1	-1	-1	-1	-1	-1	-1	-1	-1	-1	-1	-1	-1	-1	-1	-1	-1	-1	-1	-1	-1	-1	-1	-1	-1	-1	-1	-1	-1	-1	-1	-1	-1	-1	-1	-1	-1	-1	-1	-1	-1	-1	-1	-1	-1	-1	-1	-1	-1	-1	-1	-1	-1	-1	-1	-1	-1	-1	-1	-1	-1	-1	-1	-1	-1	-1	-1	-1	-1	-1	-1	-1	-1	-1	-1	-1	-1	-1	-1	-1	-1	-1	-1	-1	-1	-1	-1	-1	-1	-1	-1	-1	-1	-1	-1	-1	-1	-1	-1	-1	-1	-1	-1	-1	-1	-1	-1	-1	-1	-1	-1	-1	-1	-1	-1	-1	-1	-1	-1	-1	-1	-1	-1	-1	-1	-1	-1	-1	-1	-1	-1	-1	-1	-1	-1	-1	-1	-1	-1	-1	-1	-1	-1	-1	-1	-1	-1	-1	-1	-1	-1	-1	-1	-1	-1	-1	-1	-1	-1	-1	-1	-1	-1	-1	-1	-1	-1	-1	-1	-1	-1	-1	-1	-1	-1	-1	-1	-1	-1	-1	-1	-1	-1	-1	-1	-1	-1	-1	-1	-1	-1	-1	-1	-1	-1	-1	-1	-1	-1	-1	-1	-1	-1	-1	-1	-1	-1	-1	-1	-1	-1	-1	-1	-1	-1	-1	-1	-1	-1	-1	-1	-1	-1	-1	-1	-1	-1	-1	-1	-1	-1	-1	-1	-1	-1	-1	-1	-1	-1	-1	-1	-1	-1	-1	-1	-1	-1	-1	-1	-1	-1	-1	-1	-1	-1	-1	-1	-1	-1	-1	-1	-1	-1	-1	-1	-1	-1	-1	-1	-1	-1	-1	-1	-1	-1	-1	-1	-1	-1	-1	-1	-1	-1	-1	-1	-1	-1	-1	-1	-1	-1	-1	-1	-1	-1	-1	-1	-1	-1	-1	-1	-1	-1	-1	-1	-1	-1	-1	-1	-1	-1	-1	-1	-1	-1	-1	-1	-1	-1	-1	-1	-1	-1	-1	-1	-1	-1	-1	-1	-1	-1	-1	-1	-1	-1	-1	-1	-1	-1	-1	-1	-1	-1	-1	-1	-1	-1	-1	-1	-1	-1	-1	-1	-1	-1	-1	-1	-1	-1	-1	-1	-1	-1	-1	-1	-1	-1	-1	-1	-1	-1	-1	-1	-1	-1	-1	-1	-1	-1	-1	-1	-1	-1	-1	-1	-1	-1	-1	-1	-1	-1	-1	-1	-1	-1	-1	-1	-1	-1	-1	-1	-1	-1	-1	-1	-1	-1	-1	-1	-1	-1	-1	-1	-1	-1	-1	-1	-1	-1	-1	-1	-1	-1	-1	-1	-1	-1	-1	-1	-1	-1	-1	-1	-1	-1	-1	-1	-1	-1	-1	-1	-1	-1	-1	-1	-1	-1	-1	-1	-1	-1	-1	-1	-1	-1	-1	-1	-1	-1	-1	-1	-1	-1	-1	-1	-1	-1	-1	-1	-1	-1	-1	-1	-1	-1	-1	-1	-1	-1	-1	-1	-1	-1	-1	-1	-1	-1	-1	-1	-1	-1	-1	-1	-1	-1	-1	-1	-1	-1	-1	-1	-1	-1	-1	-1	-1	-1	-1	-1	-1	-1	-1	-1	-1	-1	-1	-1	-1	-1	-1	-1	-1	-1	-1	-1	-1	-1	-1	-1	-1	-1	-1	-1	-1	-1	-1	-1	-1	-1	-1	-1	-1	-1	-1	-1	-1	-1	-1	-1	-1	-1	-1	-1	-1	-1	-1	-1	-1	-1	-1	-1	-1	-1	-1	-1	-1	-1	-1	-1	-1	-1	-1	-1	-1	-1	-1	-1	-1	-1	-1	-1	-1	-1	-1	-1	-1	-1	-1	-1	-1	-1	-1	-1	-1	-1	-1	-1	-1	-1	-1	-1	-1	-1	-1	-1	-1	-1	-1	-1	-1	-1	-1	-1	-1	-1	-1	-1	-1	-1	-1	-1	-1	-1	-1	-1	-1	-1	-1	-1	-1	-1	-1	-1	-1	-1	-1	-1	-1	-1	-1	-1	-1	-1	-1	-1	-1	-1	-1	-1	-1	-1	-1	-1	-1	-1	-1	-1	-1	-1	-1	-1	-1	-1	-1	-1	-1	-1	-1	-1	-1	-1	-1	-1	-1	-1	-1	-1	-1	-1	-1	-1	-1	-1	-1	-1	-1	-1	-1	-1	-1	-1	-1	-1	-1	-1	-1	-1	-1	-1	-1	-1	-1	-1	-1	-1	-1	-1	-1	-1	-1	-1	-1	-1	-1	-1	-1	-1	-1	-1	-1	-1	-1	-1	-1	-1	-1	-1	-1	-1	-1	-1	-1	-1	-1	-1	-1	-1	-1	-1	-1	-1	-1	-1	-1	-1	-1	-1	-1	-1	-1	-1	-1	-1	-1	-1	-1	-1	-1	-1	-1	-1	-1	-1	-1	-1	-1	-1	-1	-1	-1	-1	-1	-1	-1	-1	-1	-1	-1	-1	-1	-1	-1	-1	-1	-1	-1	-1	-1	-1	-1	-1	-1	-1	-1	-1	-1	-1	-1	-1	-1	-1	-1	-1	-1	-1	-1	-1	-1	-1	-1	-1	-1	-1	-1	-1	-1	-1	-1	-1	-1	-1	-1	-1	-1	-1	-1	-1	-1	-1	-1	-1	-1	-1	-1	-1	-1	-1	-1	-1	-1	-1	-1	-1	-1	-1	-1	-1	-1	-1	-1	-1	-1	-1	-1	-1	-1	-1	-1	-1	-1	-1	-1	-1	-1	-1	-1	-1	-1	-1	-1	-1	-1	-1	-1	-1	-1	-1	-1	-1	-1	-1	-1	-1	-1	-1	-1	-1	-1	-1	-1	-1	-1	-1	-1	-1	-1	-1	-1	-1	-1	-1	-1	-1

Fig. 10. Agroclimatic conditions during the future spring barley grain filling period (11th day after heading to maturity) at Zaragoza as projected by four models for 2031–50, for two emission scenarios (RCPs 4.5 and 8.5) and two cultivar groups. The values for the advanced (–10, –20) and delayed (+10, +20) sowing dates indicate the projected change from the current sowing date (absolute values in given the units). Green = positive changes, red = negative changes. The intensity of the color highlights the magnitude of the change. Color-coding was done for each indicator individually except for the proportions of hot days (25/28/31) which were colored as a group and so were the durations of hot spells.

during the baseline nor during the future periods water deficit days occurred at DND.

For *HEL*, the projections showed an increase in water deficit days of, on average, 5%. For this site, fewer water deficit days were projected for the early cultivars and early sowing dates as compared to their late counter parts (Fig. S11). However, in absolute terms all these differences amounted to about one day at most. There was no single best S°C combination.

3.7. Climate model uncertainty

In general, the projections of the models from the GCM ensemble showed some deviations. The projections of *GFDL-ESM2M* were always more conservative (less change) than those of the other GCMs. For example, the projected shifts of heading and maturity dates were smaller as compared to the other models, but the direction of the change was mostly the same (Fig. 3). The temperature change projections from the baseline to the future by *GFDL-ESM2M* were also smaller than those of the other climate models (see Fig. 5).

Regarding drought, *IPSL-CM5A-LR* sometimes projected worse conditions than the other models (e.g. Figs. 5 and 6). Overall, the models deviated by at most 10 mm regarding rainfall (Fig. S12 and 13) and up to 10% regarding the proportions of dry days. The projections for dry spell durations diverged by up to 3 days while the projections for water deficit days only deviated slightly between the models. Regarding the projections for t_{mean} the models deviated by up to 1.5 °C. The projections for the different hot days showed the largest discrepancies reaching values of up to 20% (at *HEL*). Even though these deviations were numerically the largest, the directions of the projected changes were mostly the same. Regarding drought the exact opposite was the case, i.e. the deviations were smaller yet the direction of change sometimes was different (see e.g. Figs. 5, 6 or Fig. 7- DND).

4. Discussion

4.1. Projected shifts of heading and maturity dates

We first examined how air temperature, the main driver for crop phenology (Craufurd and Wheeler, 2009), was projected to change in the future spring barley growing season, then analyzed resultant effects on the phenological development of early and late heading cultivars. For

all sites along the European transect, the models projected higher ambient temperatures for 2031–50 under RCP4.5, and even more so under RCP8.5, than in the baseline period. Previously, projections for Finland have shown a temperature increase of about 1.7 °C (RCP4.5; 1.6 °C RCP8.5) for the summer months (March–August) in 2040–60 (Ruosteenoja et al., 2016). For mid-century, models have projected an increase of 1.3 °C (RCP4.5; 1.4 °C RCP8.5) of Scotland's annual mean temperature (Harkness et al., 2020 and supplement thereof) and seasonal mean temperature increments of approximately 1 °C (RCP4.5, 1.1 °C RCP8.5) for the Mediterranean (Barredo et al., 2018; Yang et al., 2019).

At all three study sites, the higher future temperatures advanced heading and maturity dates by one to three weeks (with sowing date as currently). Other studies report similar respective advancements for Northern, Central (e.g. Olesen et al., 2012), and Southern Europe (Moriondo and Bindi, 2007; Trnka et al., 2014). Warmer temperatures accelerate plant growth and development by facilitating a faster accumulation of the thermal time necessary for completing each growth stage (Craufurd and Wheeler, 2009; Harkness et al., 2020).

We confirmed the known impact of sowing date shifts on crop development (e.g. Siebert and Ewert, 2012): The more sowing was advanced the earlier heading and maturity occurred in 2031–50, because earlier sowing leads to a gain in available thermal time (Gouache et al., 2012). When sowing is delayed, the growth period is moved to warmer days (Fig. 2; Trnka et al., 2004), where now crop development benefits from the higher temperatures (Craufurd and Wheeler, 2009). This explains why even with delayed sowing, heading and maturity were still projected to occur earlier in 2031–50.

4.2. Projected agroclimatic conditions without sowing date adaptation

At the northern sites, heading and grain filling in 2031–50 were hotter and drier than in the baseline period, which is consistent with the literature. Projections for early summer in Finland have shown an increase of hot days ($t_{max} > 28$ °C) (Trnka et al., 2011b; Rötter et al., 2013) and further reductions of spring precipitation leading to more dry days (Trnka et al., 2011b; Rötter et al., 2013; Ruosteenoja et al., 2018). In Scotland, the annual number of hot days with $t_{max} > 25$ °C is expected to increase and, in general, summers in the northern UK are projected to get drier, yet the projections for some regions differ (Gosling, 2014; Harkness et al., 2020; Hanlon et al., 2021). According to the normalized

Helsinki										
Cultivar group		Early					Late			
Sowing time		-20	-10	0	+10	+20	-20	-10	0	+10
Indicator	RCP									
Sum of precipitation (mm)	4.5	35.5 (+/-3.7)								52.67 (+/-5.51)
	8.5	33.33 (+/-6.66)			51.67 (+/-4.51)					
Prop. of dry days (%)	4.5	71 (+/-2)								
	8.5	72 (+/-4)			63 (+/-4)					
Dry spell duration (d)	4.5		9 (+/-1)							
	8.5									
Tmean (°C)	4.5	17.62 (+/-0.74)								19.87 (+/-0.32)
	8.5	18.05 (+/-0.88)								20.27 (+/-0.21)
Tsum acc. (°C)	4.5	370 (+/-15)								
	8.5	379 (+/-18)								
Prop. of hot days_25 (%)	4.5									44 (+/-5)
	8.5									
Prop. of hot days_28 (%)	4.5									13 (+/-6)
	8.5									17 (+/-4)
Prop. of hot days_31 (%)	4.5									2 (+/-3)
	8.5									
Duration hot spell_25 (d)	4.5									7 (+/-1)
	8.5									
Duration hot spell_28 (d)	4.5									1 (+/-2)
	8.5									2 (+/-1)
Duration hot spell_31 (d)	4.5									
	8.5									

Zaragoza										
Cultivar group		Early					Late			
Sowing time		-20	-10	0	+10	+20	-20	-10	0	+10
Indicator	RCP									
Sum of precipitation (mm)	4.5	16.25 (+/-2.63)								26 (+/-1.41)
	8.5									
Prop. of dry days (%)	4.5	79 (+/-4)						69 (+/-8)		
	8.5	75 (+/-3)								
Dry spell duration (d)	4.5	11 (+/-1)						9 (+/-2)		
	8.5									8 (+/-2)
Tmean (°C)	4.5	11.5 (+/-0.27)								14.47 (+/-0.44)
	8.5	11.4 (+/-0.16)								14.47 (+/-0.45)
Tsum acc. (°C)	4.5	242 (+/-6)								304 (+/-9)
	8.5	240 (+/-3)								304 (+/-10)
Prop. of hot days_25 (%)	4.5	4 (+/-2)								19 (+/-7)
	8.5	6 (+/-4)								18 (+/-7)
Prop. of hot days_28 (%)	4.5	1 (+/-1)								7 (+/-3)
	8.5	2 (+/-2)								7 (+/-5)
Prop. of hot days_31 (%)	4.5	0 (+/-0)								2 (+/-2)
	8.5									
Duration hot spell_25 (d)	4.5									3 (+/-0)
	8.5	0 (+/-1)								2 (+/-1)
Duration hot spell_28 (d)	4.5									
	8.5									
Duration hot spell_31 (d)	4.5									
	8.5									

Fig. 11. Maximum (dark blue) and minimum (light blue) indicator values as projected by at least three models for the spring barley heading period (10th day pre- to 10 days post- heading) in 2031–50 for two emission scenarios (RCPs 4.5 and 8.5) at Helsinki and Zaragoza when sowing time shift and cultivar choice are combined. The values are the means of all models projecting the maximum (or minimum) value for this particular sowing x cultivar choice combination. The standard deviation (+/-) is shown.

precipitation index (calculated for three-month periods) summer (June–August) precipitation in East Scotland is projected to decline by about 10%, and dry days in the ATN zone (Atlantic North, Metzger et al., 2012), where DND is located, are projected to increase (Trnka et al., 2011b; also see Fig. S7). In contrast, Harkness et al. (2020) found that especially on the East coast of Scotland, conditions during the reproductive period of cereals (June/July) will likely remain rather favorable.

Higher mean temperatures and more hot days characterized heading in 2031–50 at ZGZ. Despite an increase of hot days during grain filling (of especially the late cultivars), the GCMs did not agree on a trend for changing t_{mean} under RCP 4.5, while for RCP8.5 they projected a slight decrease of t_{mean} (0.3 °C, mean of all models projecting the same change, i.e. HadGEM2_ES, IPSL-CM5A-LR, MIROC-ESM-CHEM).

On the one hand, for the South of Europe, hot days with $t_{\text{max}} > 30$ °C and > 34 °C are expected to occur more frequently during the cereal growing season, especially in spring and early summer (Cammarano et al., 2019a; Yang et al., 2019), and the probability of encountering heat stress during grain filling is expected to increase in the future (Trnka et al., 2014). However, the temperature-induced acceleration of phenology can prevent a crop from encountering heat stress. Warmer temperatures advance phenological stages and thereby shift them into a

new climatic window with different ambient conditions (Moriondo and Bindi, 2007; Rezaei et al., 2015). For instance, Rezaei et al. (2015) found that, by growing under cooler conditions during future heading periods, which commence earlier, wheat can avoid heat stress that would otherwise occur during the reproductive phase. Possibly, this mechanism took effect for grain filling at ZGZ, which was projected to start and end about two weeks earlier than in the baseline (Fig. 4). However, with an increasing number of hot days, as projected by the models, one would naturally expect an overall increase in t_{mean} . Presumably, much cooler days (ZGZ is one of the cooler Mediterranean sites) very early in the advanced future grain filling period compensated for the higher number of warmer days that occurred later (also see Section 4.4).

The model ensemble projected less precipitation for heading in 2031–50 at ZGZ. In general, southern Europe faces a high risk of increasing drought (Cramer et al., 2018) entailing unusually dry conditions before and after anthesis (Trnka et al., 2014). Projections of reduced amounts of rainfall (Cammarano et al., 2019a; Yang et al., 2019), more dry days, and longer dry spells are reported (Lehtonen et al., 2014). For grain filling at ZGZ, the GCMs projected decreasing amounts of rainfall, while the proportion of dry days and the duration of dry spells also decreased. Naturally, one would expect a decrease in rainfall

Helsinki										Zaragoza											
Cultivar group		Early					Late			Cultivar group		Early					Late				
Sowing time		-20	-10	0	+10	+20	-20	-10	0	+10	+20	Sowing time		-20	-10	0	+10	+20			
Indicator	RCP											Indicator	RCP								
Sum of precipitation (mm)	4.5											Sum of precipitation (mm)	4.5	45.67 (+/-1.53)					34.25 (+/-5.85)		
	8.5												8.5								
Prop. of dry days (%)	4.5											Prop. of dry days (%)	4.5								
	8.5												8.5	72 (+/-6)							
Dry spell duration (d)	4.5											Dry spell duration (d)	4.5								
	8.5						9 (+/-1)						8.5								
Tmean (°C)	4.5						20.1 (+/-0.45)					Tmean (°C)	4.5	13.55 (+/-0.34)					17.5 (+/-0.52)		
	8.5	19.83 (+/-0.4)											8.5	13.5 (+/-0.27)					17.75 (+/-0.47)		
Grain filling duration (d)	4.5	24 (+/-2)										Grain filling duration (d)	4.5	37 (+/-1)					25 (+/-1)		
	8.5	24 (+/-2)											8.5	37 (+/-0)					25 (+/-1)		
Prop of hot days_25 (%)	4.5						36 (+/-17)					Prop of hot days_25 (%)	4.5	14 (+/-5)					41 (+/-7)		
	8.5												8.5	14 (+/-6)					44 (+/-6)		
Prop of hot days_28 (%)	4.5	5 (+/-5)					14 (+/-8)					Prop of hot days_28 (%)	4.5	5 (+/-2)					21 (+/-6)		
	8.5	12 (+/-6)											8.5	5 (+/-4)					24 (+/-6)		
Prop of hot days_31 (%)	4.5	1 (+/-1)										Prop of hot days_31 (%)	4.5	1 (+/-2)					8 (+/-5)		
	8.5	2 (+/-2)											8.5	1 (+/-2)					9 (+/-7)		
Duration hot spell_25 (d)	4.5						6 (+/-2)					Duration hot spell_25 (d)	4.5	2 (+/-2)					6 (+/-1)		
	8.5												8.5	3 (+/-1)					6 (+/-1)		
Duration hot spell_28 (d)	4.5											Duration hot spell_28 (d)	4.5								
	8.5												8.5								
Duration hot spell_31 (d)	4.5											Duration hot spell_31 (d)	4.5								
	8.5												8.5								

Fig. 12. Maximum (dark blue) and minimum (light blue) indicator values as projected by at least three models for the spring barley grain filling period (11th day after heading to maturity) in 2031–50 for two emission scenarios (RCPs 4.5 and 8.5) at Helsinki and Zaragoza when sowing time shift and cultivar choice are combined. The values are the means of all models projecting the maximum (or minimum) value for this particular sowing x cultivar choice combination. The standard deviation (+/-) is shown.

to be accompanied by an increase in dry days and dry spells (Polade et al., 2014). It is important to note that the projected changes of the drought indicators at ZGZ were of a very small magnitude (Table 5) and, as mentioned above, the grain filling period was shifted to a new climatic window. The absolute values (Table 5) show that the overall amount of rainfall decreased only slightly and, due to a strong advancement, the grain filling period escaped two dry days (also see Section 4.4).

Table 5

Rainfall conditions during the spring barley grain filling period in 2031–50 as projected for Zaragoza by four models (multi-model mean, ISI-MIP2b dataset for two emission scenarios (RCPs 4.5 and 8.5). For comparison the baseline values are shown as well (1981–2010).

Time slice	Cultivar group	Duration grain filling period (days)	Precipitation (mm)	Proportion of dry days (%)	No. of dry days	Duration of longest dry spell (days)
1981–2010	early	34	53	74	25	12
	late	27	41	76	20	10
2031–50, RCP 4.5	early	33	43	70	23	11
	late	27	36	67	18	9
2031–50, RCP 8.5	early	33	42	69	23	11
	late	27	38	67	18	9

anthesis than late flowering ones (Semenov, 2009). A similar effect can be achieved with earlier sowing. Advancing sowing reduces the risk of entering heat stress in summer and allows the plant to take advantage of cooler temperatures early in the season (Sacks et al., 2010; Olesen et al., 2011). For example, Cammarano et al. (2019a) found that GCMs projected fewer hot days with $t_{\max} > 34^{\circ}\text{C}$ for the mid-century reproductive period of early-sown as compared to late-sown barley. This effect became evident at each study site along our transect: temperature conditions during heading and grain filling were coolest for the earliest sowing date and hottest for the latest one. Consequently, the coolest conditions prevailed for early cultivars sown 20 days earlier and the hottest for late cultivars sown later (for most sites 20 days later).

One exception occurred for the grain filling period at *HEL* under RCP4.5, where the greatest number of hot days with $t_{\max} \geq 25^{\circ}\text{C}$ (and the longest corresponding hot spell) were projected for late cultivars sown as currently (L 0) and the fewest for late cultivars sown 20 days later (L+20). That was due to overlapping heading and grain filling periods. The projected heading period of L+ 20 ended when L+ 0 were already 15 days into grain filling. Logically, part of the hot days that occurred at the end of heading of L+ 20, was already part of grain filling of L+ 0. Therefore, we counted maximum hot days for L+ 0 (see illustration in Fig. S6).

4.3.2. Drought stress adaptation

Against our expectations, for *HEL* the GCMs projected the driest heading and grain filling conditions for the early sowing dates/cultivars (except for grain filling under RCP8.5 where more precipitation was projected for the early cultivars). Heading was also driest for the earliest cultivar combined with the early sowing dates. The dry conditions for early heading in 2031–50 were possibly due to the early summer (June) droughts characteristic of Finland (Peltonen-Sainio et al., 2021; Fig. S7 and Fig. 4). Climate warming advances the snowmelt, which usually contributes notably to the soil moisture content in spring. Low soil moisture, coinciding with a strong temperature and solar radiation increase after the winter, creates dry conditions in early summer (Ruosteenoja et al., 2018). Depending on the models utilized, these early summer droughts could not only be maintained (Ylhäisi et al., 2010), but also even aggravated in the future by further reductions in precipitation (Ruosteenoja et al., 2018), and dry days could become more frequent (Trnka et al., 2011b; Rötter et al., 2013). Contrarily, other models project slight increases in precipitation (Ylhäisi et al., 2010; Peltonen-Sainio et al., 2021).

At *DND*, only cultivar choice had an effect on ambient growth conditions. For RCP4.5, the models projected less drought stress during heading and grain filling of the early cultivars making them a viable option for drought avoidance (Trnka et al., 2014). However, under RCP8.5, both key growth periods were drier for the early cultivars. The drier conditions (−10.5%, i.e. 4 mm rainfall; mean of the three models that predict the same direction of change) during the 10-day earlier heading period could have been due to unfavorable rainfall distribution or uncertainties related to rainfall predictions (also see Section 4.6). The duration of the grain filling periods in 2031–50 varied between the cultivar groups. The reason for the “drier conditions” (+3 dry days (= 2%), longer dry spell (+2 days)) projected for the early cultivars, likely, was not aggravated climatic conditions, but rather the longer grain filling duration (+3 days) caused by cooler temperatures (Craufurd and Wheeler, 2009). Overall, the advantage that early cultivars had over the late ones under RCP4.5 was rather small, possibly because drought conditions at this particular site as projected for 2031–50 were not as severe as suggested by other projections for larger areas of the UK (Gosling, 2014; Hanlon, 2021). Harkness et al. (2020) found that the severity of drought during future reproductive growth, occurring in June/July, is projected to decrease at various locations in the UK. Especially, on the East coast of Scotland, conditions could remain rather favorable in terms of drought; instead, heavy rainfall could become more relevant.

For *ZGZ*, we had expected more favorable conditions for the early cultivars (Rötter et al., 2013; Donatelli et al., 2015; Yang et al., 2019) and early sowing dates (Garrido et al., 2011; Yang et al., 2019). However, the heading period in 2031–50 was drier for early sowing dates/cultivars and most severe for early cultivars sown 20 days earlier. Grain filling also took place during a drier period when sowing was advanced. There was a tendency for less drought stress for late cultivars sown on different dates, but no clear picture emerged. Our results could be due to the difficulties that GCMs have in capturing the rainfall patterns of the Mediterranean, which are characterized by a high unreliability and a high variability (Dubrovský et al., 2014; Cammarano et al., 2019a, 2021).

During grain filling of the early cultivars, the sum of rainfall was higher, but more dry days and a longer dry spell occurred as compared to the late cultivars (especially under RCP. 8.5). This probably resembles a few high rainfall events that were followed by multiple dry days. Projections show a decreasing number of cyclones for the future, while the associated rainfall intensity of individual cyclones increases (van der Wiel and Bintanja, 2021). It has to be noted though that the changes in dry days and dry spells were within the order of a few days only (Fig. 8, Fig. S9). The possibility of these results being due to model error cannot be ruled out (see also the model uncertainty presented in Fig. S12 and 13).

4.4. Limits to adaptation

At northern European sites, the earliest sowing date is restricted by late spring frosts, the sufficiency of solar radiation, and the interval needed for soil thawing and drying, i.e. the time until the field is accessible to heavy machinery (Kaukoranta and Hakala, 2008; Olesen et al., 2011). Increments in winter precipitation induced by climate change have been shown to delay the first day of soil workability (Cooper et al., 1997). If sowing is postponed for too long, one might miss the optimal combination of temperature and soil moisture for germination (Peltonen-Sainio, 2012) and the vegetative growth period would get too short (Kaukoranta and Hakala, 2008).

In the Mediterranean, plant growth mainly relies on water stored in the soil. Early plant growth benefits from delayed sowing because larger quantities of stored soil water are available, however, at later growth stages the risk of entering periods of terminal stress increases. Consequently, finding the perfect sowing window is complex: One has to sow late enough to benefit from a well-filled soil water depot, yet not too late, as that entails the risk of terminal stress. Logically, sowing should be done early enough to avoid terminal stress, but not too early as one would risk damaging late frosts around heading (Cammarano et al., 2019a, 2021).

Choosing the right cultivar calls for the consideration of more factors than just stress avoidance. With higher temperatures the growing season gets shorter, limiting the amount of radiation the plant can intercept and the amount of biomass it can produce. In that case, early-flowering cultivars, which anyhow reduce their vegetative growth early to initiate reproductive growth, would produce even less biomass (Ludwig and Asseng, 2010; Shavrukov et al., 2017). This can be counteracted by growing late-flowering cultivars, which accumulate more biomass due to slower growth and have a longer grain filling period as they mature later. In case of terminal drought, however, the faster development of the early cultivars is advantageous as their earlier grain filling period occurs during cooler and wetter days before detrimental drought conditions occur. The predicament of early cultivars being beneficial under drying climates, but late ones being preferable under warming climates can only be solved by breeding new cultivars that have higher thermal requirements and heat and drought stress tolerance traits (Ludwig and Asseng, 2010; Fatima et al., 2020).

4.5. Linking and interpreting the indicators

As the projected conditions were only presented as direction changes, i.e. hotter or drier, and respective magnitudes were displayed as proportional values (in the figures), further quantifying those changes increases the understanding of the projected stress severity.

From the absolute indicator values (Fig. S8 and 9) one can see, for example, that projected climate change itself plus the two adaptation options modified the amount of precipitation during heading across all sites, on average by at most 15 mm (mean of the 3–4 GCMs agreeing on the same direction of the change calculated per cultivar group). Precipitation during the future grain filling period deviated from the baseline by at most 50 mm, while the different adaptation options altered rainfall by a maximum of about 10 mm. The absolute number of dry days and the dry spell duration varied by a maximum of about 3 (heading) and 5 (grain filling) days.

Stress severity obviously depends on the baseline conditions: At *DND*, 138 mm and at *ZGZ*, 41 mm of rainfall were projected for grain filling of the late cultivars in the baseline period. At both sites future rainfall under RCP4.5 was reduced (–29%, i.e. 40 mm, at *DND* and –13%, i.e. 5 mm, at *ZGZ*; values are model means) but actual drought stress was worse at *ZGZ*. Previous research for the Mediterranean has already shown a projected worsening of the currently existing water scarcity for the future, through further precipitation decrements and temperature increments (Cramer et al., 2018; Harmanly and Malek, 2019).

Understanding the risk of these altered conditions for plants and identifying useful adaptation options requires the additional consideration of ecophysiological aspects, for example, the distribution of dry days (and warm days) over the growing season. An in-depth analysis thereof was beyond the scope of this paper. Such interactions need quantitative assessments e.g. with dynamic crop simulation models (Rötter et al., 2011; White et al., 2011). Our study only allows for assumptions regarding warm- or dry-day distribution (Table S5). Rainfall distribution matters, as possible benefits from increasing rainfall amounts can be offset by a simultaneously increasing variability in distribution (Fishman, 2016; Lesk et al., 2020) and because the pre-exposure to any stress can affect the plant's response to subsequent drought stress (Jacques et al., 2021) or heat stress (Bäurle, 2016). High intensity rainfall events and/or high daily totals have been shown to affect barley growth and yield e.g. through waterlogging, soil erosion or root anoxia (e.g. Rötter et al., 2018).

To create a general picture of a potentially changing agroclimate our indicator set mainly represented atmospheric conditions. Heat as an indicator does not include soil or canopy temperature conditions, and drought indicators only refer to meteorological drought which is strictly defined as the water deficit due to an imbalance between precipitation and evaporation. Lack of rainfall can translate into a soil moisture deficit and a shortage of water available to the plant entailing negative consequences for crop growth and yield (Liu et al., 2016). While it is still valid to focus on meteorological drought as it is the prerequisite for agricultural drought (Dai et al., 2018), ultimately, soil conditions are the crucial factor. Favorable loam or clay soils can serve as a buffer if sufficient water has been stored earlier in the season, while unfavorable coarse and shallow soils cannot (e.g. Ludwig and Asseng, 2010; Rötter et al., 2013). Whether sandy or clay soils are beneficial for drought survival also depends on the cultivar used (early vs late flowering), the expected type of drought (e.g. early or terminal), and on ambient temperatures. Especially in Mediterranean areas, where crop production relies on stored soil moisture, the soil type is crucial (Ludwig and Asseng, 2010).

To illustrate this effect of soil we calculated the number of water deficit days for the heading and grain filling periods for the three study sites. In absolute terms, for 2031–50 for *HEL*, the models projected at most 5 water deficit days, and even less to none for *DND* and *ZGZ*. Only in *HEL*, early sowing and using early cultivars reduced the exposure to

water deficit days by 1 day. These small numbers were due to the fact that we only examined the comparatively small time windows of heading and grain filling. From the baseline to the future, the other drought indicators signaled an increase in dry conditions at *DND*, but no actual water deficit days occurred, probably due to the high water storage capacity of the soil at *DND* (Ludwig and Asseng, 2010).

The water balances for *HEL* and *ZGZ* did not reflect the observations made earlier with the indicators, e.g. the early summer droughts at *HEL* or the reduction in rainfall during heading at *ZGZ*. Even though the water storage capacities of both soils were lower, possibly the projected rainfall deficits were not severe enough to deplete the soil water storage to such an extent that actual agricultural drought would occur.

However, we draw all of these conclusions with some caution due to various uncertainties arising from different sources. Obviously, the water balance calculation builds on the projection of rainfall amounts and patterns which have their own amount of uncertainty (see 4.6). Adding to this, the calculation of evapotranspiration itself was subjected to uncertainty. The transmissivity of solar radiation (i.e. cloudiness), a crucial factor in the evapotranspiration process (Allen et al., 1998), was estimated internally by the software package, which could have over- or under-estimated the real values. Analyzing physiological concepts like evapotranspiration in greater depths requires the use of crop simulation models.

Another important factor, yet beyond the scope of this paper, is the coupled occurrence of heat and drought stress. It causes the plant's individual stress responses to occur simultaneously exacerbating potential damage (Suzuki et al., 2014). For example, in *HEL* about 60% of the 23-day grain filling period were dry days and about 40% warm days with $t_{\max} \geq 25^\circ\text{C}$; therefore, coinciding heat and drought stress could have been possible.

4.6. Strengths and limitations of the study

We characterized projected climate change conditions for spring barley cultivation along a European transect in great detail. Agroclimatic indicators have been used to describe projected production conditions in general and for specific crops in time slices of the past and the future at locations in Finland (Rötter et al., 2012, 2013 – spring barley), Scotland (Rivington et al., 2013 – general; Harkness et al., 2020 – winter wheat; Arnell and Freeman, 2021 – general), Spain (Camarano et al., 2019a – barley), Central and Eastern Europe (Trnka et al., 2011a, 2011b; – general; Eitzinger et al., 2013 – application of calculated indicators to barley in case studies; Lüttger and Feike, 2018 – winter wheat), the US (Troy et al., 2015 – corn, soy, spring and winter wheat, rice), and locations all across Europe (Trnka et al., 2014 – winter wheat) or the world (Zhu and Troy, 2018; Vogel et al., 2019 – corn, spring wheat, rice, soybean). Most of these studies were based on a larger temporal and spatial scale than ours. None of them simultaneously examined the agroclimatic conditions during the two most important growth stages of contrasting spring barley cultivars and describe how two of the most detrimental stress conditions could potentially change in the future with and without the implementation of adaptation options. The results of the few wheat agroclimatology studies cannot be readily transferred to barley even though these cereals are quite similar. Barley has a greater early growth vigor (López-Castañeda et al., 1995) than wheat and another study showed greater photoperiod sensitivity for spring barley as compared to winter wheat (Volk and Bugbee, 1991). Most importantly, barley is more drought hardy than wheat and is therefore suitable for harsher environments, like the dry areas of the Mediterranean (López-Castañeda et al., 1995; Zarei et al., 2021). Our study provides a unique overview of projected agroclimatic conditions for spring barley production in 2031–50 and possible effects of different adaptation options; nonetheless, it has its limitations.

Projections for precipitation are subject to much larger inter – model (GCM) variability than temperature projections (Dubrovský et al., 2014; van der Wiel and Bintanja, 2021) and precipitation itself is a highly

variable parameter as shown for Finland (Ylhäisi et al., 2010), Scotland (Harkness et al., 2020), and the Mediterranean (Dono et al., 2016; Cammarano et al., 2019a, 2021). In some cases, the GCMs in our study not only diverged numerically but also, especially for drought, in the direction of the change. This gave rise to the sometimes unclear results regarding drought stress.

The use of bias-corrected output of GCMs instead of regional climate models possibly influenced the results (Dieng et al., 2018). However, since the main focus was the difference between cultivars in combination with shifting sowing dates and not the accuracy of climate change projections, the choice of climate models was not decisive here.

Describing heat stress conditions worked sufficiently well with the simplistic approach of calculating agroclimatic indicators, as these results were generally consistent with the literature. For the characterization of drought, this approach might have been a bit too simplistic. To better capture drought related processes including soil factors in greater detail than possible with simple soil water balances and to better link heat and drought effects, agroclimatic indicators should be coupled with crop models (e.g. see Rötter et al., 2012; Rötter et al., 2013; Gouache et al., 2012; Donatelli et al., 2015; Harkness et al., 2020).

Complementing the set of indicators with heavy rainfall (Harkness et al., 2020) and frost (Hakala et al., 2012) or considering increasing atmospheric CO₂ concentrations (Swann et al., 2016) would have been worthwhile, but was beyond the scope of this study.

5. Conclusion

At three contrasting sites along a climatic transect, from northern (Helsinki, Dundee) to southern (Zaragoza) Europe, heading and maturity dates projected for 2031–50 occurred up to three weeks earlier than in the baseline period 1981–2010. According to selected agroclimatic indicators, at the northern sites the conditions during these projected heading and grain filling periods were drier and hotter than in the baseline period. At all three sites, heat stress during future heading and grain filling was avoided by advancing both stages as much as possible, i.e. by sowing early cultivars as early as possible. At Helsinki, delaying the heading period allowed spring barley to escape the early summer droughts that would usually occur during heading. At Dundee, under RCP4.5, early cultivars were exposed to slightly wetter growing conditions than the late cultivars. At Zaragoza, fewer yet more intense rainfall events occurred during grain filling of the early cultivars. Despite the simplicity of the agroclimatic indicator approach, our study provides a unique overview of agroclimatic conditions for heading and grain filling as projected for 2031–50 and shows the possible effects of different adaptation options. To the best of our knowledge, this is the first study describing projected changes for 2031–50 for two of the most detrimental stress conditions during the two most important growth stages of contrasting spring barley cultivars, as well as the effects of possible adaptation options. To find the most suitable combination of adaptation options for different target environments based on quantitative estimates of associated yield changes, the analysis with agroclimatic indicators should be extended with crop simulation models. A major effort to build, evaluate, and apply advanced genotype-specific barley simulation models for all important cultivation environments in Europe is currently underway by the BARISTA project (<https://www.barleyhub.org/barista/>).

Declaration of Competing Interest

The authors declare that they have no known competing financial interests or personal relationships that could have appeared to influence the work reported in this paper.

Data Availability

Data will be made available on request.

Acknowledgements

MA, GBM, NCRF, AHS and RPR have received funding from the European Union's Horizon 2020 research and innovation program under grant agreement No 771134. The project BARISTA was carried out under the ERA-NET Cofund SusCrop (Grant number: N°771134) being part of the Joint Programming Initiative on Agriculture, Food Security and Climate Change (FACCE-JPI). We acknowledge the support of Ernesto Igartua (CSIC), Alessandro Tondelli (CREA), Andrea Visioni (ICARDA) and Bill Thomas (JHI) who organized data collection at the field sites and helped us during the data organization process. We thank all the staff that was involved in collecting the data for the ClimBar project.

Appendix A. Supporting information

Supplementary data associated with this article can be found in the online version at [doi:10.1016/j.fcr.2022.108768](https://doi.org/10.1016/j.fcr.2022.108768).

References

- Allen, R.G., Pereira, L.S., Raes, D., Smith, M., 1998. Crop evapotranspiration - Guidelines for computing crop water requirements. FAO Irrigation and drainage paper 56.
- Alqudah, A.M., Schnurbusch, T., 2014. Awn primordium to tipping is the most decisive developmental phase for spikelet survival in barley. *FPB* 41 (4), 424–436. <https://doi.org/10.1071/FP13248>.
- Arnell, N.W., Freeman, A., 2021. The effect of climate change on agro-climatic indicators in the UK. *Clim. Change* 165 (40), 1–26. <https://doi.org/10.1007/s10584-021-03054-8>.
- Barredo, J.I., Mauri, A., Caudullo, G., Dosio, A., 2018. Assessing shifts of Mediterranean and arid climates under RCP4.5 and RCP8.5 climate projections in Europe. *Pure Appl. Geophys.* 175 (11), 3955–3971. <https://doi.org/10.1007/s00024-018-1853-6>.
- Bäurle, I., 2016. Plant Heat Adaptation: priming in response to heat stress: [version1; referees: 2 approved]. *F1000Research* 5 (694), 1–5. <https://doi.org/10.12688/f1000research.7526.1>.
- Bojanowski, J., 2016. Package "sirad". Functions for Calculating Daily Solar Radiation and Evapotranspiration.
- Brereton, J.C., McGowan, M., Dawkins, T., 1986. The relative sensitivity of spring barley, spring field beans and sugar beet crops to soil compaction. *Field Crops Res.* 13, 223–237.
- Cammarano, D., Ceccarelli, S., Grando, S., Romagosa, I., Benbelkacem, A., Akar, T., Al-Yassin, A., Pecchioni, N., Francia, E., Ronga, D., 2019a. The impact of climate change on barley yield in the Mediterranean basin. *Eur. J. Agron.* 106, 1–11. <https://doi.org/10.1016/j.eja.2019.03.002>.
- Cammarano, D., Ronga, D., Francia, E., Akar, T., Al-Yassin, A., Benbelkacem, A., Grando, S., Romagosa, I., Stanca, A.M., Pecchioni, N., 2021. Genetic and management effects on barley yield and phenology in the Mediterranean basin. *Front Plant Sci.* 12, 655406. <https://doi.org/10.3389/fpls.2021.655406>.
- Chmielewski, F.-M., 2013. Phenology in agriculture and horticulture. In: Schwartz, M.D. (Ed.), *Phenology: An integrative environmental science*, 2 ed., Springer. <https://doi.org/10.1007/978-94-007-6925-0>.
- Cooper, G., McGeachan, M.B., Vinten, A., 1997. The influence of a changed climate on soil workability and available workdays in Scotland. *J. Agric. Eng. Res* 68 (3), 253–269. <https://doi.org/10.1006/jaer.1997.0204>.
- Copernicus Climate Change Service, 2019. Agrometeorological indicators from 1979 up to 2019 derived from reanalysis. Version 1. 0. <https://doi.org/10.24381/CDS.6C68C9BB>.
- Cossani, C.M., Slafer, G.A., Savin, R., 2009. Yield and biomass in wheat and barley under a range of conditions in a Mediterranean site. *Field Crops Res* 112 (2–3), 205–213. <https://doi.org/10.1016/j.fcr.2009.03.003>.
- Cramer, W., Guiot, J., Fader, M., Garrahou, J., Gattuso, J.-P., Iglesias, A., Lange, M.A., Lionello, P., Llasat, M.C., Paz, S., Peñuelas, J., Snoussi, M., Toreti, A., Tsimplis, M.N., Xoplaki, E., 2018. Climate change and interconnected risks to sustainable development in the Mediterranean. *Nat. Clim. Change* 8 (11), 972–980. <https://doi.org/10.1038/s41558-018-0299-2>.
- Craufurd, P.Q., Wheeler, T.R., 2009. Climate change and the flowering time of annual crops. *J. Exp. Bot.* 60 (9), 2529–2539. <https://doi.org/10.1093/jxb/erp196>.
- Dai, A., Zhao, T., Chen, J., 2018. Climate Change and Drought: A Precipitation and Evaporation Perspective. *Curr. Clim. Change Rep.* 4 (3), 301–312. <https://doi.org/10.1007/s40641-018-0101-6>.
- Dieng, D., Laux, P., Smiatek, G., Heinzeller, D., Bliefernicht, J., Sarr, A., Gaye, A.T., Kunstmann, H., 2018. Performance analysis and projected changes of agroclimatic indices across West Africa based on high-resolution regional climate model simulations. *J. Geophys. Res. Atmos.* 110 (1), 77. <https://doi.org/10.1029/2018JD028536>.
- Donatelli, M., Srivastava, A.K., Duveiller, G., Niemeyer, S., Fumagalli, D., 2015. Climate change impact and potential adaptation strategies under alternate realizations of climate scenarios for three major crops in Europe. *Environ. Res. Lett.* 10 (7), 75005. <https://doi.org/10.1088/1748-9326/10/7/075005>.

- Dono, G., Cortignani, R., Dell'Unto, D., Deligios, P., Doro, L., Lacetera, N., Mula, L., Pasqui, M., Quaresima, S., Vitali, A., Roggero, P.P., 2016. Winners and losers from climate change in agriculture: Insights from a case study in the Mediterranean basin. *Agric. Syst.* 147, 65–75. <https://doi.org/10.1016/j.agry.2016.05.013>.
- Dubrovský, M., Hayes, M., Duce, P., Trnka, M., Svoboda, M., Zara, P., 2014. Multi-GCM projections of future drought and climate variability indicators for the Mediterranean region. *Reg. Environ. Change* 14 (5), 1907–1919. <https://doi.org/10.1007/s10113-013-0562-z>.
- Edwards, J., 2010. Barley growth and development. *NSW-Gov. Procrops* 82.
- Eitzinger, J., Trnka, M., Semerádová, D., Thaler, S., Svobodová, E., Hlavinka, P., Šiška, B., Takáč, J., Malatinská, L., Nováková, M., Dubrovský, M., Žalud, Z., 2013. Regional climate change impacts on agricultural crop production in Central and Eastern Europe – hotspots, regional differences and common trends. *J. Agric. Sci.* 151 (6), 787–812. <https://doi.org/10.1017/S0021859612000767>.
- FAO, 2020. FAOSTAT. Food and Agriculture Organization of the United Nations. (<http://www.fao.org/faostat/en>).
- Fatima, Z., Ahmed, M., Hussain, M., Abbas, G., Ul-Allah, S., Ahmad, S., Ahmed, N., Ali, M.A., Sarwar, G., Haque, E.U., Iqbal, P., Hussain, S., 2020. The fingerprints of climate warming on cereal crops phenology and adaptation options. *Sci. Rep.* 10 (1), 18013. <https://doi.org/10.1038/s41598-020-74740-3>.
- Fishman, R., 2016. More uneven distributions overturn benefits of higher precipitation for crop yields. *Environ. Res. Lett.* 11 (2), 24004. <https://doi.org/10.1088/1748-9326/11/2/024004>.
- Frieler, K., Lange, S., Piontek, F., Rey, C.P.O., Schewe, J., Warszawski, L., Zhao, F., Chini, L., Denvil, S., Emanuel, G., Geiger, T., Halladay, K., Hurr, G., Mengel, M., Murakami, D., Ostberg, S., Popp, A., Riva, R., Stevanovic, M., Suzuki, T., Volkholz, J., Burke, E., Ciais, P., Ebi, K., Eddy, T.D., Elliott, J., Galbraith, E., Goshing, S.N., Hattermann, F., Hickler, T., Hinkel, J., Hof, C., Huber, V., Jägermeyr, J., Krysanova, V., Marcé, R., Müller Schmied, H., Mouratiadou, I., Pierson, D., Tittensor, D.P., Vautard, R., van Vliet, M., Biber, M.F., Betts, R.A., Bodirsky, B.L., Deryng, D., Frothing, S., Jones, C.D., Lotze, H.K., Lotze-Campen, H., Sahajpal, R., Thonicke, K., Tian, H., Yamagata, Y., 2017. Assessing the impacts of 1.5 °C global warming – simulation protocol of the Inter-Sectoral Impact Model Intercomparison Project (ISI-MIP2b). *Geosci. Model Dev.* 10 (12), 4321–4345. <https://doi.org/10.5194/gmd-10-4321-2017>.
- Gao, Y., Leung, L.R., Lu, J., Masato, G., 2015. Persistent cold air outbreaks over North America in a warming climate. *Environ. Res. Lett.* 10 (4), 44001. <https://doi.org/10.1088/1748-9326/10/4/044001>.
- Garrido, A., Rey, D., Ruiz-Ramos, M., Mínguez, M.I., 2011. Climate change and crop adaptation in Spain: -consistency of regional climate models. *Clim. Res.* 49 (3), 211–227. <https://doi.org/10.1354/cr01029>.
- Gosling, R., 2014. Assessing the impact of projected climate change on drought vulnerability in Scotland. *Hydrol. Res.* 45 (6), 806–816. <https://doi.org/10.2166/nh.2014.148>.
- Gouache, D., Le Bris, X., Bogard, M., Deudon, O., Pagé, C., Gate, P., 2012. Evaluating agronomic adaptation options to increasing heat stress under climate change during wheat grain filling in France. *Eur. J. Agron.* 39, 62–70. <https://doi.org/10.1016/j.eja.2012.01.009>.
- Hakala, K., Jauhainen, L., Himanen, S.J., Rötter, R., Salo, T., Kahiluoto, H., 2012. Sensitivity of barley varieties to weather in Finland. *J. Agric. Sci.* 150 (2), 145–160. <https://doi.org/10.1017/S0021859611000694>.
- Hanlon, H.M., Bernie, D., Carigi, G., Lowe, J.A., 2021. Future changes to high impact weather in the UK. *Clim. Change* 166 (50), 2–23. <https://doi.org/10.1007/s10584-021-03100-5>.
- Harkness, C., Semenov, M.A., Areal, F., Senapati, N., Trnka, M., Balek, J., Bishop, J., 2020. Adverse weather conditions for UK wheat production under climate change. *Agric. J. Meteorol.* 282–283, 107862. <https://doi.org/10.1016/j.agrformet.2019.107862>.
- Harmanny, K.S., Malek, Z., 2019. Adaptations in irrigated agriculture in the Mediterranean region: an overview and spatial analysis of implemented strategies. *Reg. Environ. Change* 19 (5), 1401–1416. <https://doi.org/10.1007/s10113-019-01494-8>.
- Hempel, S., Frieler, K., Warszawski, L., Schewe, J., Piontek, F., 2013. A trend-preserving bias correction – the ISI-MIP approach. *Earth Syst. Dynam.* 4 (2), 219–236. <https://doi.org/10.5194/esd-4-219-2013>.
- Ito, R., Shioyama, H., Nakaegawa, T., Takayabu, I., 2019. Uncertainties in climate change projections covered by the ISIMIP and CORDEX model subsets from CMIP5. *Geosci. Model Dev.* 13 (3) <https://doi.org/10.5194/gmd-2019-143>.
- Jacott, C.N., Boden, S.A., 2020. Feeling the heat: developmental and molecular responses of wheat and barley to high ambient temperatures. *J. Exp. Bot.* 71 (19), 5740–5751. <https://doi.org/10.1093/jxb/era326>.
- Jacques, C., Salon, C., Barnard, R.L., Vernoud, V., Prudent, M., 2021. Drought stress memory at the plant cycle level: A review. *Plants (Basel, Switz.)* 10 (1837), 1–13. <https://doi.org/10.3390/plants10091873>.
- Kadam, N.N., Xiao, G., Melgar, R.J., Bahuguna, R.N., Quinones, C., Tamilselvan, A., Prasad, P.V.V., Jagadish, K.S., 2014. Agronomic and physiological responses to high temperature, drought, and elevated CO₂ interactions in cereals. In: Sparks, D.L. (Ed.), *Advances in agronomy*, vol. 127. Elsevier, Amsterdam, pp. 111–156. <https://doi.org/10.1016/B978-0-12-800131-8.00003-0>.
- Kahiluoto, H., Kaseva, J., Balek, J., Olesen, J.E., Ruiz-Ramos, M., Gobin, A., Kersebaum, K.C., Takáč, J., Ruget, F., Ferrise, R., Bezak, P., Capellades, G., Dibari, C., Mäkinen, H., Nendel, C., Ventrella, D., Rodríguez, A., Bindi, M., Trnka, M., 2019. Decline in climate resilience of European wheat. *Proc. Natl. Acad. Sci. USA* 116 (1), 123–128. <https://doi.org/10.1073/pnas.1804387115>.
- Kaukoranta, T., Hakala, K., 2008. Impact of spring warming on sowing times of cereal, potato and sugar beet in Finland. *AFS* 17 (2), 165. <https://doi.org/10.2137/145960608785328198>.
- Kovats, R.S., Valentini, L.M., Bouwer, E., Georgopoulou, D., Jacob, E.M., Rounsevell, M., Soussana, J.-F., 2014. Europe. In: Barros, V.R., Field, C.B., Dokken, D.J., Mastrandrea, M.D., Mach, K.J., Bilir, T.E., Chatterjee, M., Ebi, K., Estrada, Y.O., Genova, R.C., Girma, B., Kissel, E.S., Levy, A.N., MacCracken, S., Mastrandrea, P.R., White, L.L. (Eds.), *Climate Change 2014: Impacts, Adaptation and Vulnerability*. Cambridge University Press, Cambridge, United Kingdom and New York, NY, USA, pp. 1267–1326. <https://doi.org/10.1017/CBO9781107415386.003>.
- Lehtonen, I., Ruosteenoja, K., Jylhä, K., 2014. Projected changes in European extreme precipitation indices on the basis of global and regional climate model ensembles. *Int. J. Climatol.* 34 (4), 1208–1222. <https://doi.org/10.1002/joc.3758>.
- Lesk, C., Coffel, E., Horton, R., 2020. Net benefits to US soy and maize yields from intensifying hourly rainfall. *Nat. Clim. Chang* 10 (9), 819–822. <https://doi.org/10.1038/s41558-020-0830-0>.
- Liu, X., Zhu, X., Pan, Y., Li, S., Liu, Y., Ma, Y., 2016. Agricultural drought monitoring: Progress, challenges, and prospects. *J. Geogr. Sci.* 26 (6), 750–767. <https://doi.org/10.1007/s11442-016-1297-9>.
- López-Castañeda, C., Richards, R.A., Farquhar, G.D., 1995. Variation in Early Vigor between Wheat and Barley. *Crop Sci.* 35, 472.
- Ludwig, F., Asseng, S., 2010. Potential benefits of early vigor and changes in phenology in wheat to adapt to warmer and drier climates. *Agric. Syst.* 103 (3), 127–136. <https://doi.org/10.1016/j.agry.2009.11.001>.
- Lüttger, A.B., Feike, T., 2018. Development of heat and drought related extreme weather events and their effect on winter wheat yields in Germany. *Theor. Appl. Climatol.* 132 (1–2), 15–29. <https://doi.org/10.1007/s00704-017-2076-y>.
- Metzger, M.J., Bunce, R.G.H., Jongman, R.H.G., Múcher, C.A., Watkins, J.W., 2005. A climatic stratification of the environment of Europe. *Glob. Ecol. Biogeogr.* 14 (6), 549–563. <https://doi.org/10.1111/J.1466-822X.2005.00190.X>.
- Metzger, M.J., Shkaruba, A.D., Jongman, R., Bunce, R., 2012. Descriptions of the European environmental zones and strata, Wageningen Alterra, Alterra Report 2281, 154 pp.
- Miroslavjević, M., Momčilović, V., Dencić, S., Mikić, S., Trkulja, D., Pržulj, N., 2018. Grain number and grain weight as determinants of triticale, wheat, two-rowed and six-rowed barley yield in the Pannonian environment. *Span. J. Agric. Res.* 16 (3), e0903. <https://doi.org/10.5424/sjar/2018163-11388>.
- Moriando, M., Bindi, M., 2007. Impact of climate change on the phenology of typical Mediterranean crops. *Ital. J. Agrometeorol.* 3, 5–12.
- Newton, A.C., Flavell, A.J., George, T.S., Leat, P., Mullholland, B., Ramsay, L., Revoredoghi, C., Russell, J., Steffenson, B.J., Swanston, J.S., Thomas, W.T.B., Waugh, R., White, P.J., Bingham, I.J., 2011. Crops that feed the world 4. Barley: a resilient crop? Strengths and weaknesses in the context of food security. *Food Sect. 3* (2), 141–178. <https://doi.org/10.1007/s12571-011-0126-3>.
- Olesen, J.E., Petersen, B.M., Bernsten, J., Hansen, S., Jamieson, P.D., Thomsen, A.G., 2002. Comparison of methods for simulating effects of nitrogen on green area index and dry matter growth in winter wheat. *Field Crops Res.* 74, 131–149.
- Olesen, J.E., Trnka, M., Kersebaum, K.-C., Skjelvåg, A.O., Seguin, B., Peltonen-Sainio, P., Rossi, F., Kozzra, J., Micale, F., 2011. Impacts and adaptation of European crop production systems to climate change. *Eur. J. Agron.* 34 (2), 96–112. <https://doi.org/10.1016/j.eja.2010.11.003>.
- Olesen, J.E., Børgesen, C.D., Elsgaard, L., Palosuo, T., Rötter, R.P., Skjelvåg, A.O., Peltonen-Sainio, P., Børjesson, T., Trnka, M., Ewert, F., Siebert, S., Brissin, N., Eitzinger, J., van Asselt, E.D., Oberforster, M., van der Fels-Klerx, H.J., 2012. Changes in time of sowing, flowering and maturity of cereals in Europe under climate change. *Food Addit. Contam. Part A Chem. Anal. Control Expo. Risk Assess.* 29 (10), 1527–1542. <https://doi.org/10.1080/19440049.2012.712060>.
- Pachauri, R.K., Mayer, L. (Eds.), 2015. Climate change 2014: Synthesis report. Contribution of Working Groups I, II and III to the 5th Assessment Report of the IPCC. Intergovernmental Panel on Climate Change, Geneva, Switzerland, 151 pp.
- Peltonen-Sainio, P., 2012. Crop production in a northern climate. *Build. Resil. Adapt. Clim. Change Agric. Sect. vol.* 23, 183–214.
- Peltonen-Sainio, P., Juvonen, J., Korhonen, N., Parkkila, P., Sorvali, J., Gregow, H., 2021. Climate change, precipitation shifts and early summer drought: An irrigation tipping point for Finnish farmers? *Clim. Risk Manag.* 33, 100334. <https://doi.org/10.1016/j.crm.2021.100334>.
- Pendergrass, A.G., Knutti, R., Lehner, F., Deser, C., Sanderson, B.M., 2017. Precipitation variability increases in a warmer climate. *Sci. Rep.* 7 (1), 17966. <https://doi.org/10.1038/s41598-017-17966-y>.
- Polade, S.D., Pierce, D.W., Cayan, D.R., Gershunov, A., Dettinger, M.D., 2014. The key role of dry days in changing regional climate and precipitation regimes. *Sci. Rep.* 4, 4364. <https://doi.org/10.1038/srep04364>.
- Porter, J.R., Gawith, M., 1999. Temperatures and the growth and development of wheat: A review. *Eur. J. Agron.* 10, 23–36.
- Reig-Gracia, F., Vicente-Serrano, S.M., Dominguez-Castro, F., Bedia-Jiménez, J., 2019. Climate Indices: Package ClimInd.
- Rezaei, E.E., Siebert, S., Ewert, F., 2015. Intensity of heat stress in winter wheat—phenology compensates for the adverse effect of global warming. *Environ. Res. Lett.* 10 (2), 24012. <https://doi.org/10.1088/1748-9326/10/2/024012>.
- Rivington, M., Matthews, K.B., Buchan, K., Miller, D.G., Bellocchi, G., Russell, G., 2013. Climate change impacts and adaptation scope for agriculture indicated by agro-meteorological metrics. *Agric. Syst.* 114, 15–31. <https://doi.org/10.1016/j.agry.2012.08.003>.
- Rötter, R.P., Palosuo, T., Pirttioja, N., Dubrovsky, M., Salo, T., Fronzek, S., Aikasalo, R., Trnka, M., Ristolainen, A., Carter, T.R., 2011. What would happen to barley

- production in Finland if global warming exceeded 4°C? A model-based assessment. *Eur. J. Agron.* 35 (4), 205–214. <https://doi.org/10.1016/j.eja.2011.06.003>.
- Rötter, R.P., Höhn, J.G., Fronzek, S., 2012. Projections of climate change impacts on crop production: A global and a Nordic perspective. *Acta Agric. Scand. - A: Anim. Sci.* 62 (4), 166–180. <https://doi.org/10.1080/09064702.2013.793735>.
- Rötter, R.P., Höhn, J., Trnka, M., Fronzek, S., Carter, T.R., Kahiluoto, H., 2013. Modelling shifts in agroclimatic and crop cultivar response under climate change. *Ecol. Evol.* 3 (12), 4197–4214. <https://doi.org/10.1002/ece3.782>.
- Rötter, R.P., Tao, F., Höhn, J.G., Palosuo, T., 2015. Use of crop simulation modelling to aid ideotype design of future cereal cultivars. *J. Exp. Bot.* 66 (12), 3463–3476. <https://doi.org/10.1093/jxb/erv098>.
- Rötter, R.P., Appiah, M., Fichtler, E., Kersebaum, K.-C., Trnka, M., Hoffmann, M.P., 2018. Linking modelling and experimentation to better capture crop impacts of agroclimatic extremes—A review. *Field Crops Res.* 221, 142–156. <https://doi.org/10.1016/j.fcr.2018.02.023>.
- Ruiz-Ramos, M., Ferrise, R., Rodríguez, A., Lorite, I.J., Bindi, M., Carter, T.R., Fronzek, S., Palosuo, T., Pirttioja, N., Baranowski, P., Buis, S., Cammarano, D., Chen, Y., Duponnois, R., Ewert, F., Gaiser, T., Hlavinka, P., Hoffmann, H., Höhn, J. G., Jurečka, F., Kersebaum, K.-C., Krzyszczak, J., Lana, M., Mechiche-Alami, A., Minet, J., Montesino, M., Nendel, C., Porter, J.R., Ruget, F., Semenov, M.A., Steinmetz, Z., Stratonovitch, P., Supit, I., Tao, F., Trnka, M., Wit, A., de, Rötter, R.P., 2018. Adaptation response surfaces for managing wheat under perturbed climate and CO₂ in a Mediterranean environment. *Agric. Syst.* 159, 260–274. <https://doi.org/10.1016/j.agry.2017.01.009>.
- Ruosteenoja, K., Jylh, K., Kämäräinen, M., 2016. Climate projections for Finland under the RCP forcing scenarios. *Geophysica* 51 (1), 17–50.
- Ruosteenoja, K., Markkanen, T., Venäläinen, A., Räisänen, P., Peltola, H., 2018. Seasonal soil moisture and drought occurrence in Europe in CMIP5 projections for the 21st century. *Clim. Dyn.* 50 (3–4), 1177–1192. <https://doi.org/10.1007/s00382-017-3671-4>.
- Sacks, W.J., Deryng, D., Foley, J.A., Ramankutty, N., 2010. Crop planting dates: an analysis of global patterns. *Glob. Ecol. Biogeogr.* 19, 607–620. <https://doi.org/10.1111/j.1466-8238.2010.00551.x>.
- Semenov, M.A., 2009. Impacts of climate change on wheat in England and Wales. *J. R. Soc. Interface* 6 (33), 343–350. <https://doi.org/10.1098/rsif.2008.0285>.
- Shavruk, Y., Kurishbayev, A., Jatayev, S., Shvidchenko, V., Zotova, L., Koekemoer, F., Groot, S., de, Soole, K., Langridge, P., 2017. Early flowering as a drought escape mechanism in plants: How can it aid wheat production? *Front. Plant Sci.* 8, 1950. <https://doi.org/10.3389/fpls.2017.01950>.
- Siebert, S., Ewert, F., 2012. Spatio-temporal patterns of phenological development in Germany in relation to temperature and day length. *Agric. Meteorol.* 152, 44–57. <https://doi.org/10.1016/j.agrformet.2011.08.007>.
- Suzuki, N., Rivero, R.M., Shulaev, V., Blumwald, E., Mittler, R., 2014. Abiotic and biotic stress combinations. *N. Phytol.* 203 (1), 32–43. <https://doi.org/10.1111/nph.12797>.
- Swann, A.L.S., Hoffman, F.M., Koven, C.D., Randerson, J.T., 2016. Plant responses to increasing CO₂ reduce estimates of climate impacts on drought severity. *PNAS* 113 (36), 10019–10024. <https://doi.org/10.1073/pnas.1604581113>.
- Taylor, K.E., 2012. An overview of CMIP5 and the experiment design. *Bull. Am. Meteor. Soc.* 93 (4), 485–498. <https://doi.org/10.1175/BAMS-D-11-00094.1>.
- Trnka, M., Dubrovsky, M., Zalud, Z., 2004. Climate change impacts and adaptation strategies in spring barley production in the Czech Republic. *Clim. Change* 64, 227–255.
- Trnka, M., Eitzinger, J., Semerádová, D., Hlavinka, P., Balek, J., Dubrovský, M., Kubu, G., Štěpánek, P., Thaler, S., Možný, M., Zalud, Z., 2011a. Expected changes in agroclimatic conditions in Central Europe. *Clim. Change* 108 (1–2), 261–289. <https://doi.org/10.1007/s10584-011-0025-9>.
- Trnka, M., Olesen, J.E., Kersebaum, K.-C., Skjelvåg, A.O., Eitzinger, J., Seguin, B., Peltonen-Sainio, P., Rötter, R.P., Iglesias, A., Orlandini, S., Dubrovsky, M., Hlavinka, P., Balek, J., Eckersten, H., Cloppet, E., Calanca, P., Gobin, A., Vučetić, V., Nejedlik, P., Kumar, S., Lalic, B., Mestre, A., Rossi, F., Kozyra, J., Alexandrov, V., Semerádová, D., Zalud, Z., 2011b. Agroclimatic conditions in Europe under climate change. *Glob. Chang. Biol.* 17 (7), 2298–2318. <https://doi.org/10.1111/j.1365-2486.2011.02396.x>.
- Trnka, M., Rötter, R.P., Ruiz-Ramos, M., Kersebaum, K.-C., Olesen, J.E., Zalud, Z., Semenov, M.A., 2014. Adverse weather conditions for European wheat production will become more frequent with climate change. *Nat. Clim. Chang* 4 (7), 637–643. <https://doi.org/10.1038/nclimate2242>.
- Troy, T.J., Kipgen, C., Pal, I., 2015. The impact of climate extremes and irrigation on US crop yields. *Environ. Res. Lett.* 10 (5), 54013. <https://doi.org/10.1088/1748-9326/10/5/054013>.
- USDA, 2020b). Source: US Department of Agriculture - (<https://ipad.fas.usda.gov/cropeexplorer/cropview/commodityView.aspx?cropid=0430000>) accessed 07/12/2020.
- USDA, 2020a. Grain: World Markets and Trade, 42 pp. October 2020, <https://usda.library.cornell.edu/concern/publications/zs25x844t?locale=en&page=3#release-items> accessed 30/10/2020.
- van der Wiel, K., Bintanja, R., 2021. Contribution of climatic changes in mean and variability to monthly temperature and precipitation extremes. *Commun. Earth Environ.* 2 (1), 1–11. <https://doi.org/10.1038/s43247-020-00077-4>.
- Vogel, E., Donat, M.G., Alexander, L.V., Meinshausen, M., Ray, D.K., Karoly, D., Meinshausen, N., Frieler, K., 2019. The effects of climate extremes on global agricultural yields. *Environ. Res. Lett.* 14 (5), 54010. <https://doi.org/10.1088/1748-9326/ab154b>.
- Volk, T., Bugbee, B., 1991. Modeling Light and Temperature Effects on Leaf Emergence in Wheat and Barley. *Crop Sci.* 31.
- Warszawski, L., Frieler, K., Huber, V., Piontek, F., Serdeczny, O., Schewe, J., 2014. The Inter-Sectoral Impact Model Intercomparison Project (ISI-MIP): project framework. *PNAS* 111 (9), 3228–3232. <https://doi.org/10.1073/pnas.1312330110>.
- White, J.W., Hoogenboom, G., Kimball, B.A., Wall, G.W., 2011. Methodologies for simulating impacts of climate change on crop production. *Field Crops Res.* 124 (3), 357–368. <https://doi.org/10.1016/j.fcr.2011.07.001>.
- Yang, C., Fraga, H., van Ieperen, W., Trindade, H., Santos, J.A., 2019. Effects of climate change and adaptation options on winter wheat yield under rainfed Mediterranean conditions in southern Portugal. *Clim. Change* 154 (1–2), 159–178. <https://doi.org/10.1007/s10584-019-02419-4>.
- Yawson, D.O., Adu, M.O., Armah, F.A., 2020. Impacts of climate change and mitigation policies on malt barley supplies and associated virtual water flows in the UK. *Sci. Rep.* 10 (1), 376. <https://doi.org/10.1038/s41598-019-57256-3>.
- Ylhäisi, J.S., Tietäväinen, H., Peltonen-Sainio, P., Venäläinen, A., Eklund, J., Räisänen, J., Jylhä, K., 2010. Growing season precipitation in Finland under recent and projected climate. *Nat. Hazards Earth Syst. Sci.* 10 (7), 1563–1574. <https://doi.org/10.5194/nhess-10-1563-2010>.
- Zadoks, J.C., Chang, T.T., Konzak, C.F., 1974. A decimal code for the growth stages of cereals.
- Zarei, A.R., Shabani, A., Mahmoudi, M.R., 2021. Susceptibility Assessment of Winter Wheat, Barley and Rapeseed to Drought Using Generalized Estimating Equations and Cross-Correlation Function. *Environ. Process.* 8, 163–197.
- Zhu, X., Troy, T.J., 2018. Agriculturally relevant climate extremes and their trends in the world's major growing regions. *Earth's Future* 6 (4), 656–672. <https://doi.org/10.1002/2017EF000687>.